

## Insight into the Boundary Layer Flows of Free Convection and Heat Transfer of Nanofluids Over a Vertical Plate using Multi-Step Differential Transformation Method

**M. G. Sobamowo\***  
Assistant Professor

**A. A. Yinusa†**  
Instructor

*This paper presents an insight into the boundary layer of free convection and heat transfer of nanofluids over a vertical plate at very low and high Prandtl number. Suitable similarity variables are used to convert the governing systems of nonlinear partial differential equations of the flow and heat transfer to systems of nonlinear ordinary differential equations which are solved using multi-step differential transformation method. The approximate analytical solutions are verified with numerical solutions. From the parametric studies, it is observed that the velocity and temperature of the nanofluid decreases and increases, respectively as the Prandtl number and volume-fraction of the nanoparticles in the base fluid increase. Also, the decrease in velocity and increase in temperature are highest in lamina shaped nanoparticle followed by platelets, cylinder, bricks and sphere shaped nanoparticles, respectively. Using a common base fluid to all the nanoparticle type, it is observed that the decrease in velocity and increase in temperature are highest  $\text{TiO}_2$  followed by  $\text{CuO}$ ,  $\text{Al}_2\text{O}_3$  and SWCNTs nanoparticles, in that order. The present study will enhance the understanding of free convection boundary-layer problems.*

**Keywords:** Free convection; Boundary layer; Heat transfer; Nanofluid; Multi-step differential transformation method.

### 1 Introduction

The flow and heat transfer characteristics of fluid over stretching plates have attracted the interest of many researchers in recent times. This is due to their several applications in engineering such as foodstuff processing, reactor fluidization, extrusion, melt spinning, glass-fibre production processes, food processing, mechanical forming processes, wire and fiber coating, cooling of metallic plates, drawing of a polymer sheet, aerodynamic, aeronautics, cooling of gas turbine rotor blades, extrusion of plastic sheets, continuous casting, rolling, annealing, and tinning of copper wires.

\* Assistant Professor, Department of Mechanical Engineering, University of Lagos, Akoka, Lagos, Nigeria, mikegbeminiyi@gmail.com

† Instructor, Department of Mechanical Engineering, University of Lagos, Akoka, Lagos, Nigeria mynotebook2010@yahoo.com

Manuscript received April 01, 2018; revised June 28, 2018; accepted July 01, 2018.

In the extrusion process, this understanding is crucial for maintenance of the surface quality of the extrudate. The coating process requires a smooth surface for the best product appearance and for such properties as low friction, transparency, and strength. As the quality of product in the extrusion processes depends considerably on the flow and heat transfer characteristics of a thin liquid film over a stretching sheet, analysis of momentum and heat transfer in such processes is essential. Therefore, in the study of free convection and heat transfer problems, the analysis of incompressible laminar flow of viscous fluid in a steady state, two-dimensional free convection boundary-layer has over the years been a common area of increasing research interests following experimental investigations of Schmidt and Beckmann [1] and the pioneering theoretical work of Ostrach et al. [2].

In their attempt to study the laminar free convection flow and heat transfer problem in (1953), Ostrach et al. [2] applied method of iterative integration to analyze free convection over a semi-infinite isothermal flat plate. The author obtained the numerical solutions for a wide range of Prandtl numbers from 0.01 to 1000 and validated their numerical results using experimental data of Schmidt and Beckmann [1]. Five years later, Sparrow and Gregg [3] presented a further study on numerical solutions for laminar free convection from a vertical plate with uniform surface heat flux. Considering the fact that the major part of low Prandtl-number boundary layer of free convection is inviscid, Lefevre [4] examined the laminar free convection of an inviscid flow from a vertical plane surface. In a further work, Sparrow and Gregg [5] developed similar solutions for free convection from a non-isothermal vertical plate.

Meanwhile, a study on fluid flow over a heated vertical plate at high Prandtl number was presented by Stewartson and Jones [6]. Due to the disadvantages in the numerical methods in the previous studies [2, 3], Kuiken [7] adopted method of matched asymptotic expansion and established asymptotic solutions for large Prandtl number free convection. In the subsequent year, the same author applied the singular perturbation method and analyzed free convection at low Prandtl numbers [8]. Also, in another work on the asymptotic analysis of the same problem, Eshghy [9] studied free-convection boundary layers at large Prandtl number while Roy [10] investigated free convection for uniform surface heat flux at high Prandtl number. With the development of asymptotic solution using perturbation method, a combined study of the effects of small and high Prandtl numbers on the viscous fluid flow over a flat vertical plate was submitted by Kuiken and Rotem [11].

However, the requirement, searching and exertness of small parameter in the equations make the perturbation methods limited in applications. Therefore, Na and Habib [12] applied parameter differentiation method to solve the free convection boundary layer problem. Few years later, Merkin [13] presented the similarity solutions for free convection on a vertical plate while Merkin and Pop [14] used finite difference method to develop numerical solutions for conjugate free convection problem of boundary-layer flow over a vertical plate. Also, Ali et al. [15] submitted a study on numerical investigation of free convective boundary layer in a viscous fluid. The various analytical and numerical studies of the past works have shown that the boundary layer problems are very difficult to solve because besides having very thin regions where there is rapid change of the fluid properties they are defined on unbounded domains. Although, analytical methods are used to solve boundary layer problems, they converge very slowly for some boundary layer problems, particularly those with very large parameters.

The numerical methods used also encounter problems in resolving the solution of the governing equations in the very thin regions and in cases where singularities or multiple solutions exist. Additionally, intensive computer time is required to solve the problem using numerical methods. Consequently, it is often costly and time consuming to get a complete curve of results with these methods. Furthermore, the numerical methods are based on discrete techniques and as a result, only the calculations of the approximate solutions for some values of time and space variables are carried out and some important phenomena of the problem can be overlooked.

Therefore, it is absolutely required that the stability and convergence analysis should be carried so as to avoid divergence or inappropriate results.

In recent times, various new mathematical techniques have been developed for providing approximate analytical solutions to nonlinear problems. These methods include Adomian decomposition method (ADM), homotopy perturbation method (HPM), variation iteration method (VIM), differential transformation method (DTM), variation of parameter method (VPM), homotopy analysis method (HAM) etc. In the quest of presenting symbolic solutions to the flow and heat transfer problem using one of the recently developed semi-analytical methods, Motsa et al. [16] adopted homotopy analysis method to solve the free convection boundary layer flow with heat and mass transfer. In another work, the authors applied spectral local linearization approach for solving the natural convection boundary layer flow [17] while Ghotbi et al. [18] developed analytical solutions to the natural convection boundary layer flow using homotopy analysis method. Although, the homotopy analysis method (HAM) is a very reliable and efficient semi-analytical technique, it suffers from a number of limiting assumptions such as the requirements that the solution ought to conform to the so-called rule of solution expression and the rule of coefficient ergodicity.

Also, the use of HAM in the analysis of linear and nonlinear equations requires the determination of auxiliary parameter which will increase the computational cost and time. Additionally, the lack of rigorous theories or proper guidance for choosing initial approximation, auxiliary linear operators, auxiliary functions, and auxiliary parameters limits the applications of HAM. Moreover, such method requires high skill in mathematical analysis and the solution comes with large number of terms.

The relative simplicity coupled with ease of applications of differential transformation method (DTM) has proven that the method is more effective than most of the other approximate analytical methods. The differential transformation method as introduced by Zhou [19] has fast gained ground as it appeared in many engineering and scientific research papers. This is because, with the applications of DTM, a closed form series solution or approximate solution can be provided for nonlinear integral and differential equations without linearization, analytical integration, restrictive assumptions, perturbation, evaluation of the Lagrangian multiplier, difficult computation for finding the Adomian polynomials and discretization or round-off error. It reduces complexity of expansion of derivatives and the computational difficulties of the other traditional or recently developed methods.

Therefore, Yu and Chen [20] applied the differential transformation method to provide approximate analytical solutions to Blasius equation. Also, Kuo [21] adopted the same method to determine the velocity and temperature profiles of the Blasius equation of forced convection problem for fluid flow passing over a flat plate. An extended work on the applications of differential transformation method to free convection boundary-layer problem of two-dimensional steady and incompressible laminar flow passing over a vertical plate was presented by the same author [22]. However, in the later work, the nonlinear coupled boundary value equations governing the flow and heat transfer processes are reduced to initial value equations by a group of transformation and the resulting coupled initial-value equations are solved by means of the differential transformation method. The reduction or the transformation of the boundary value problems to the initial value problems was carried out due to the fact that the developed systems of nonlinear differential equations contain an unbounded domain of infinite boundary conditions. Moreover, in order to obtain the numerical solutions that are valid over the entire large domain of the problem, Ostrach et al. [2] has earlier estimated the values of  $f''(0)$  and  $\theta'(0)$  during the analysis of the developed systems of fully coupled nonlinear ordinary differential equations. Following the Ostrach et al's approach, most of the subsequent solutions provided in literature [3, 9, 10, 12, 14, 15, 21, and 22] were based on the estimated boundary conditions given by Ostrach et al [1].

Additionally, there are the limitations of power series solutions to small domain values of the independent variable(s). Consequently, the DTM solutions diverge for some differential equations that extremely have nonlinear behaviors or have boundary-conditions at infinity. However, in some recent studies, the use of power series methods coupled with Padé-approximant technique have shown to be very effective way of developing accurate analytical solutions to nonlinear problems of large or unbounded domain problems of infinite boundary conditions. Therefore, in a recent work, Rashidi et al. [23] applied differential transformation method coupled with Padé-approximant technique to develop a novel analytical solution for mixed convection about an inclined flat plate embedded in a porous medium. Although, the application of Padé-approximant technique with power series method increases the rate of convergence and the radius of convergence of power series solution, it comes with large volume of calculations and computations. Therefore, in some recent studies on boundary-layer flows [24-39], the nonlinear equations are solved by new semi-analytical schemes which include the multi-step differential transform method (MDTM). The main advantage of MDTM is that it can be applied directly to nonlinear differential equations of infinite boundary conditions without the use of after-treatment techniques and domain transformation techniques. By applying the MDTM, the interval of convergence for the series solution is increased. The MDTM is treated as an algorithm in a sequence of intervals for finding accurate approximate solutions for systems of differential equations.

The previous studies on the problem under investigation are based on the flow of viscous fluid as shown in the above review. To the best of the author's knowledge, a study on the influence of nanoparticle shape, size and type on the free convection boundary-layer flow and heat transfer of nanofluids over a vertical plate at low and high Prandtl numbers using multi-step differential transformation method has not been carried out. Therefore, the present study demonstrates the application of multi-step differential transformation method to develop approximate analytical solutions for the free convection boundary-layer flow and heat transfer of nanofluids of different nano-size particles over a vertical plate at low and high Prandtl numbers. Another novelty of the present study is displayed in the development of approximate analytical solutions for the free convection boundary layer problem without the use of the estimated boundary conditions  $f''(0)$  and  $\theta'(0)$  during the analysis of the problem.

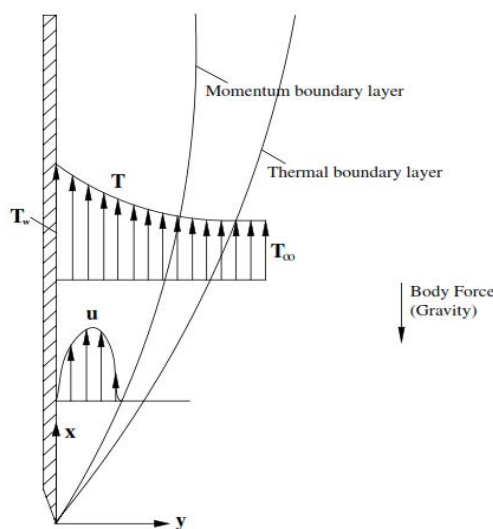


**Figure 1** Velocity and temperature profiles in free convection flow over a vertical plate [20]

## 2 Problem Formulation and Mathematical analysis

Consider a laminar free-convection flow of an incompressible nanofluid over a vertical plate parallel to the direction of the generating body force as shown in Fig. (1). Assuming that the flow in the laminar boundary layer is two-dimensional and steady, the equations for continuity and motion are given as

$$\frac{\partial u}{\partial x} + \frac{\partial v}{\partial y} = 0 \quad (1)$$

$$\rho_{nf} \left( u \frac{\partial u}{\partial x} + v \frac{\partial u}{\partial y} \right) = \mu_{nf} \frac{\partial^2 u}{\partial y^2} + g (\rho \beta)_{nf} (T - T_{\infty}) \quad (2)$$





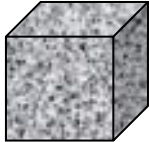
$$(\rho c_p)_{nf} \left( u \frac{\partial T}{\partial x} + v \frac{\partial T}{\partial y} \right) = k_{nf} \frac{\partial^2 T}{\partial y^2} \quad (3)$$

Assuming no slip conditions, the appropriate boundary conditions are given as

$$u = 0, \quad v = 0, \quad T = T_s \quad \text{at} \quad y = 0 \quad (4a)$$

$$u = 0, \quad T = T_w, \quad \text{at} \quad y \rightarrow \infty \quad (4b)$$

**Table 1** The values of different shapes of nanoparticles [28, 29]

S/N	Name	Shape	Shape factor ( $m$ )	Sphericity( $\psi$ )
1	Sphere		3.0	1.000
2	Platelet		5.7	0.526
3	Cylinder		4.8	0.625
4	Lamina		16.2	0.185
5	Brick		3.7	0.811

Where the various physical and thermal properties in the Eq. (1-3) are given as

$$\rho_{nf} = \rho_f (1 - \phi) + \rho_s \phi \quad (5a)$$

$$(\rho c_p)_{nf} = (\rho c_p)_f (1 - \phi) + (\rho c_p)_s \phi \quad (5b)$$

$$(\rho \beta)_{nf} = (\rho \beta)_f (1 - \phi) + (\rho \beta)_s \phi \quad (5c)$$

$$\mu_{nf} = \frac{\mu_f}{(1 - \phi)^{2.5}} \quad (5c)$$

$$k_{nf} = k_f \left[ \frac{k_s + (m - 1)k_f - (m - 1)\phi(k_f - k_s)}{k_s + (m - 1)k_f + \phi(k_f - k_s)} \right] \quad (6)$$

where  $m$  in the above Hamilton Crosser's model in Eq. (6) is the shape factor which numerical values for different shapes are given in Table (1). It should be noted that the shape factor relates with the sphericity by  $m = \frac{3}{\lambda}$ , where  $\lambda$  is the sphericity (the ratio of the surface area of the sphere and the surface area of the real particles with equal volumes) [28, 29]. For sphericity of sphere, platelet, cylinder, laminar and brick are 1.000, 0.526, 0.625, 0.185 and 0.811, respectively. The Hamilton Crosser's model becomes a Maxwell-Garnett's model, when the shape factor of the nanoparticle,  $m=3$ . Table (2) and (3) present the physical and thermal properties of the base fluid and the nanoparticles, respectively. SWCNTs mean single-walled carbon nanotubes. Going back to Eq. (1), (2) and (3) and if one introduces a stream function,  $\psi(x, y)$  such that

$$u = \frac{\partial \psi}{\partial y}, \quad v = -\frac{\partial \psi}{\partial x}, \quad (7)$$

and use the following similarity and dimensionless variables

$$\eta = \left[ \frac{\rho_f^2 (g \beta_f (T_w - T_\infty))}{4 \mu_f^2 x} \right]^{1/4} y, \quad \psi = \frac{4 \mu_f}{\rho_f} \left[ \frac{\rho_f^2 (g \beta_f (T_w - T_\infty)) x^3}{4 \mu_f^2} \right]^{1/4} f(\eta), \quad (8)$$

$$\theta = \frac{T - T_\infty}{T_w - T_\infty}, \quad Pr = \frac{\mu_f c_p}{k_f},$$

**Table 2** Physical and thermal properties of the base fluid [28-33]

Base fluid	$\rho$ (kg/m <sup>3</sup> )	$c_p$ (J/kgK)	$k$ (W/mK)
Pure water	997.1	4179	0.613
Ethylene Glycol	1115	2430	0.253
Engine oil	884	1910	0.144
Kerosene	783	2010	0.145

**Table 3** Physical and thermal properties of nanoparticles [28-33]

Nanoparticles	$\rho$ (kg/m <sup>3</sup> )	$c_p$ (J/kgK)	$k$ (W/mK)
Copper (Cu)	8933	385	401
Aluminum oxide (Al <sub>2</sub> O <sub>3</sub> )	3970	765	40
SWCNTs	2600	42.5	6600
Silver (Ag)	10500	235.0	429
Titanium dioxide (TiO <sub>2</sub> )	4250	686.2	8.9538
Copper (II) Oxide (CuO)	783	540	18

one arrives at fully coupled third and second orders ordinary differential equations

$$f'''(\eta) + (1-\phi)^{2.5} \left\{ \left[ (1-\phi) + \phi \left( \frac{\rho_s}{\rho_f} \right) \right] \left( 3f(\eta)f''(\eta) - 2(f'(\eta))^2 \right) + \left[ (1-\phi) + \phi \left[ (\rho\beta)_s / (\rho\beta)_f \right] \right] \theta(\eta) \right\} = 0 \quad (9)$$

$$\theta''(\eta) + 3 \left[ \frac{1}{\left[ (1-\phi) + \phi \left[ (\rho C_p)_s / (\rho C_p)_f \right] \right]} \left[ \frac{k_s + (m-1)k_f - (m-1)\phi(k_f - k_s)}{k_s + (m-1)k_f + \phi(k_f - k_s)} \right] \right] Prf\eta\theta'(\eta) = 0 \quad (10)$$

and the boundary conditions as

$$\begin{aligned} f = 0, \quad f' = 0, \quad \theta = 1, \quad \text{when } \eta = 0 \\ f' = 0, \quad \theta = 0, \quad \text{when } \eta = \infty \end{aligned} \quad (11)$$

It should be noted that for a viscous fluid which does not have nanoparticles, the nanoparticle volume fraction is zero i.e.  $\phi=0$  and then one recovers the earlier models [2-15] from Eq. (9) and (10) which are

$$f''' + 3ff'' - 2(f')^2 + \theta = 0 \quad (12)$$

$$\theta'' + 3Prf\theta' = 0 \quad (13)$$

and the boundary conditions remain the same as in Eq. (11)

### 3 Basic Concepts of differential transform method

The relatively new semi-analytical method, differential transformation method introduced by Zhou [19] has proven proved very effective in providing highly accurate solutions to differential equations, difference equation, differential-difference equations, fractional differential equation, pantograph equation and integro-differential equation. Therefore, this method is applied to the present study. The basic definitions and the operational properties of the method are as follows:

If  $u(t)$  is analytic in the domain T, then the function  $u(t)$  will be differentiated continuously with respect to time  $t$ .

$$\frac{d^p u(t)}{dt^p} = \varphi(t, p) \text{ for all } t \in T \quad (14)$$

for  $t = t_i$ , then  $\varphi(t, p) = \varphi(t_i, p)$ , where  $p$  belongs to the set of non-negative integers, denoted as the  $p$ -domain. We can therefore write Eq. (14) as

$$U(p) = \varphi(t_i, p) = \left[ \frac{d^p u(t)}{dt^p} \right]_{t=t_i} \quad (15)$$

Where  $U_p$  is called the spectrum of  $u(t)$  at  $t = t_i$ . Expressing  $u(t)$  in Taylor's series as

$$u(t) = \sum_p \left[ \frac{(t-t_i)^p}{p!} \right] U(p) \quad (16)$$

Where Equ. (14) is the inverse of  $U(k)$  us symbol 'D' denoting the differential transformation process and combining (15) and (16), we have

$$u(t) = \sum_{p=0}^{\infty} \left[ \frac{(t-t_i)^p}{p!} \right] U(p) = D^{-1}U(p) \quad (17)$$

#### 4 Basic Concepts of Multi-Step differential transform method

The limitation of classical DTM is shown when is being used for solving differential equations with the boundary conditions at infinity i.e. the obtained series solution through the DTM for such equation with the boundary condition become divergent. Besides that, generally, power series solutions are not useful for large values of the independent variable. In order to overcome this shortcoming, the multi-step DTM is developed. The basic concepts of the multi-step DTM for solving non-linear initial-value problem is presented as follows,

$$u(t, f, f', \dots, f^{(h)}) = 0, \quad (18)$$

subject to the initial conditions

$$f^{(k)}(0) = c_k, \quad k = 0, 1, \dots, h-1. \quad (19)$$

Let  $[0, T]$  be the interval over which we want to find the solution of the initial value problem of Eq. (18). In actual application of the DTM, the approximate solution of the initial value problem of Eq. (18) can be expressed by the following finite series:

$$f(t) = \sum_{m=0}^M a_m t^m \quad t \in [0, T]. \quad (20)$$

The multi-step approach introduces a new idea for constructing the approximate solution. Assume that the interval  $[0, T]$  is divided into  $N$  subintervals  $[t_{i-1}, t_i]$ ,  $i = 1, 2, \dots, N$  of equal step size  $H = T/N$  by using the nodes  $t = iH$ . The main idea of the multi-step DTM is as follows. First, we apply the DTM to Eq. (18) over the interval  $[0, t_1]$ , we will obtain the following approximate solution,

$$f_1(t) = \sum_{m=0}^K a_{1m} t^m \quad t \in [0, t_1], \quad (21)$$



**Table 4** Operational properties of differential transformation method

S/N	Function	Differential transform
1	$u(t) \pm v(t)$	$U(p) \pm V(p)$
2	$\alpha u(t)$	$\alpha U(p)$
3	$\frac{du(t)}{dt}$	$(p+1)U(p+1)$
4	$u(t)v(t)$	$\sum_{r=0}^p V(r)U(p-r)$
5	$u^m(t)$	$\sum_{r=0}^p U^{m-1}(r)U(p-r)$
6	$\frac{d^n u(t)}{dx^n}$	$(p+1)(p+2)\cdots(p+n)U(p+n)$
7	$\sin(\omega t + \alpha)$	$\frac{\omega^p}{p!} \sin\left(\frac{\pi p}{2!} + \alpha\right)$
8	$\cos(\omega t + \alpha)$	$Z(p) = \frac{\omega^p}{p!} \cos\left(\frac{\pi p}{2!} + \alpha\right)$

Using the initial conditions  $f^{(k)}(0) = c_k$ . For  $i \geq 2$  and at each subinterval  $[t_{i-1}, t_i]$  we will use the initial conditions  $f_i^{(k)}(t_{i-1}) = f_{i-1}^{(k)}(t_{i-1})$  and apply the DTM to Eq. (18) over the interval  $[t_{i-1}, t_i]$ , where  $t_0$  in Eq. (15) is replaced by  $t_{i-1}$ . The process is repeated and generates a sequence of approximate solution  $f_i(t)$ ,  $i = 1, 2, \dots, N$ , for the solution  $f(t)$ ,

$$f_i(t) = \sum_{m=0}^K a_{im} (t - t_{i-1})^m, \quad t \in [t_i, t_{i+1}], \quad (22)$$

Where  $M = K \cdot N$ . In fact, the multi-step DTM assumes the following solution:

$$f(t) = \begin{cases} f_1(t), & t \in [0, t_1] \\ \vdots \\ f_i(t), & t \in [t_i, t_{i+1}] \\ \vdots \\ f_N(t), & t \in [t_{N-1}, t_N] \end{cases} \quad (23)$$

which shows that there is a separate function for every sub domain. Following the above definition, it could be stated that the multi-step DTM for every sub-domain is defined as

$$F_i(m) = \frac{H^m}{m!} \left[ \frac{d^m u(t)}{dt^m} \right]_{t=t_i} \quad (24)$$

The inverse multi-step DTM is

$$f_i(t) = \sum_{m=0}^{\infty} \left[ \frac{(t-t_i)^m}{m!} \right] F_i(m) \quad (25)$$

The new algorithm, multi-step DTM is simple for computational performance for all values of  $H$ . It is easily observed that if the step size  $H = T$ , then the multi-step DTM reduces to the classical DTM. Using the operational properties of the differential transformation method, the differential transformation of the governing differential Eq. (9) is given as

$$\begin{aligned} & (p+1)(p+2)(p+3)F(p+3) \\ & + (1-\phi)^{2.5} \left\{ \left[ (1-\phi) + \phi \left( \frac{\rho_s}{\rho_f} \right) \right] \left[ 3 \sum_{l=0}^p (p-l+1)(p-l+2)F(l)F(p-l+2) \right] \right. \\ & \left. - 2 \sum_{l=0}^p (l+1)(p-l+1)F(l+1)F(p-l+1) \right\} \\ & + \left[ (1-\phi) + \phi \left[ (\rho\beta)_s / (\rho\beta)_f \right] \right] \Theta(p) \quad (26) \end{aligned}$$

Equivalently, we can write the recursive relation for Eq. (26) in DTM domain as

$$F(p+3) = \frac{(1-\phi)^{2.5}}{(p+1)(p+2)(p+3)} \left\{ \left[ (1-\phi) + \phi \left( \frac{\rho_s}{\rho_f} \right) \right] \left[ 2 \sum_{l=0}^p (l+1)(p-l+1)F(l+1)F(p-l+1) \right] \right. \\ \left. - 3 \sum_{l=0}^p (p-l+1)(p-l+2)F(l)F(p-l+2) \right\} - \left[ (1-\phi) + \phi \left[ (\rho\beta)_s / (\rho\beta)_f \right] \right] \Theta(p) \quad (27)$$

For the Eq.(10), we have the recursive relation in differential transform domain as

$$\begin{aligned} & (p+1)(p+2)\Theta(p+2) + \\ & \left\{ 3Pr \left[ \frac{1}{\left[ (1-\phi) + \phi \left[ (\rho C_p)_s / (\rho C_p)_f \right] \right]} \left[ \frac{k_s + (m-1)k_f - (m-1)\phi(k_f - k_s)}{k_s + (m-1)k_f + \phi(k_f - k_s)} \right] \right] \right. \\ & \left. \times \sum_{l=0}^p (l+1)\Theta(l+1)F(p-l) \right\} = 0 \quad (28) \end{aligned}$$

which can be written as

$$\Theta(p+2) = \frac{-3Pr}{(p+1)(p+2)} \left\{ \left[ \frac{1}{\left[ (1-\phi) + \phi \left[ (\rho C_p)_s / (\rho C_p)_f \right] \right]} \left[ \frac{k_s + (m-1)k_f - (m-1)\phi(k_f - k_s)}{k_s + (m-1)k_f + \phi(k_f - k_s)} \right] \right] \right. \\ \left. \times \sum_{l=0}^p (l+1)\Theta(l+1)F(p-l) \right\} \quad (29)$$

Also, recursive relation for the boundary conditions in Eq.(12) are

$$\begin{aligned}
 F(p) = 0 &\Rightarrow F(0) = 0, \quad (p+1)F(p+1) = 0 \Rightarrow F(1) = 0, \quad \theta(p) = 1 \Rightarrow \theta(0) = 1, \\
 F(2) &= \frac{a}{2}, \quad \theta(1) = b,
 \end{aligned}
 \tag{30}$$

Where  $a$  and  $b$  are unknown constants which will be found later. It should be noted that the transformations which included “ $a$ ” and “ $b$ ” are established from values of  $f''(0)=a$  and  $\theta'(0)=b$ . From Eq. (28), we have the following boundary conditions in differential transform domain

$$F(0) = 0, \quad F(1) = 0, \quad \theta(0) = 1, \quad F(2) = \frac{a}{2}, \quad \theta(1) = b \tag{31}$$

Using  $p=0, 1, 2, 3, 4, 5, 6, 7\dots$  in the above recursive relations in Eq. (28), we arrived at

$$\begin{aligned}
 F[3] &= \frac{-(1-\phi)^{2.5}}{6} \left\{ (1-\phi) + \phi \left[ (\rho\beta)_s / (\rho\beta)_f \right] \right\} \\
 F[4] &= \frac{-(1-\phi)^{2.5}}{24} \left\{ (1-\phi) + \phi \left[ (\rho\beta)_s / (\rho\beta)_f \right] \right\} b
 \end{aligned}$$

$$F[5] = \frac{(1-\phi)^{2.5}}{120} \left\{ (1-\phi) + \phi \left( \frac{\rho_s}{\rho_f} \right) \right\} a^2$$

$$F[6] = 0$$

$$\begin{aligned}
 F[7] &= \frac{(1-\phi)^{2.5}}{210} \left( \begin{aligned} &2 \left\{ (1-\phi) + \phi \left( \frac{\rho_s}{\rho_f} \right) \right\} \left[ -\left( \frac{1}{3} \right) (1-\phi)^{2.5} \left\{ (1-\phi) + \phi \left[ (\rho\beta)_s / (\rho\beta)_f \right] \right\} ab \right. \\ &\quad \left. + \left( \frac{1}{4} \right) (1-\phi)^5 \left\{ (1-\phi) + \phi \left[ (\rho\beta)_s / (\rho\beta)_f \right] \right\}^2 \right] \\ &- 3 \left\{ (1-\phi) + \phi \left( \frac{\rho_s}{\rho_f} \right) \right\} \left[ \frac{-7(1-\phi)^{2.5}}{24} \left\{ (1-\phi) + \phi \left[ (\rho\beta)_s / (\rho\beta)_f \right] \right\} ab \right. \\ &\quad \left. + \frac{(1-\phi)^5}{6} \left\{ (1-\phi) + \phi \left[ (\rho\beta)_s / (\rho\beta)_f \right] \right\}^2 \right] \\ &+ \frac{\left\{ (1-\phi) + \phi \left[ (\rho\beta)_s / (\rho\beta)_f \right] \right\} Pr}{8} \left\{ \frac{1}{\left[ (1-\phi) + \phi \left[ (\rho c_p)_s / (\rho c_p)_f \right] \right]} \cdot \right. \\ &\quad \left. \left[ \frac{k_s + (m-1)k_f - (m-1)\phi(k_f - k_s)}{k_s + (m-1)k_f + \phi(k_f - k_s)} \right] \right\} ab \end{aligned} \right)
 \end{aligned}$$

$$F[8] = \frac{(1-\phi)^{2.5}}{336} \left( \begin{aligned} & 2 \left\{ (1-\phi) + \phi \left( \frac{\rho_s}{\rho_f} \right) \right\} \left[ \frac{(1-\phi)^{2.5}}{12} \left\{ (1-\phi) + \phi \left( \frac{\rho_s}{\rho_f} \right) \right\} a^3 \right. \right. \\ & \quad \left. \left. + \frac{(1-\phi)^5}{6} \left\{ (1-\phi) + \phi \left[ (\rho\beta)_s / (\rho\beta)_f \right] \right\}^2 b \right] \right. \\ & - 3 \left\{ (1-\phi) + \phi \left( \frac{\rho_s}{\rho_f} \right) \right\} \left[ \frac{11(1-\phi)^{2.5}}{20} \left\{ (1-\phi) + \phi \left( \frac{\rho_s}{\rho_f} \right) \right\} a^3 \right. \\ & \quad \left. \left. + \frac{(1-\phi)^5}{8} \left\{ (1-\phi) + \phi \left[ (\rho\beta)_s / (\rho\beta)_f \right] \right\}^2 b \right] \right. \\ & - \left[ \frac{\left\{ (1-\phi) + \phi \left[ (\rho\beta)_s / (\rho\beta)_f \right] \right\}^2 Pr (1-\phi)^{2.5}}{40} \right] \left\{ \frac{1}{\left[ (1-\phi) + \phi \left[ (\rho c_p)_s / (\rho c_p)_f \right] \right]} \cdot \right. \\ & \quad \left. \left[ \frac{k_s + (m-1)k_f - (m-1)\phi(k_f - k_s)}{k_s + (m-1)k_f + \phi(k_f - k_s)} \right] \right\} b \end{aligned} \right)$$

$$F[9] = \frac{(1-\phi)^{2.5}}{540} \left( \begin{aligned} & 2 \left\{ (1-\phi) + \phi \left( \frac{\rho_s}{\rho_f} \right) \right\} \left[ -\frac{(1-\phi)^5}{24} \left\{ (1-\phi) + \phi \left[ (\rho\beta)_s / (\rho\beta)_f \right] \right\} \left\{ (1-\phi) + \phi \left( \frac{\rho_s}{\rho_f} \right) \right\} a^2 \right. \right. \\ & \quad \left. \left. + \frac{(1-\phi)^5}{36} \left\{ (1-\phi) + \phi \left[ (\rho\beta)_s / (\rho\beta)_f \right] \right\}^2 b^2 \right] \right. \\ & - 3 \left\{ (1-\phi) + \phi \left( \frac{\rho_s}{\rho_f} \right) \right\} \left[ -\frac{13(1-\phi)^5}{360} \left\{ (1-\phi) + \phi \left[ (\rho\beta)_s / (\rho\beta)_f \right] \right\} \left\{ (1-\phi) + \phi \left( \frac{\rho_s}{\rho_f} \right) \right\} a^2 \right. \\ & \quad \left. \left. + \frac{(1-\phi)^5}{48} \left\{ (1-\phi) + \phi \left[ (\rho\beta)_s / (\rho\beta)_f \right] \right\}^2 b^2 \right] \right. \\ & - \left[ \frac{\left\{ (1-\phi) + \phi \left[ (\rho\beta)_s / (\rho\beta)_f \right] \right\}^2}{240} \right] Pr \left\{ \frac{1}{\left[ (1-\phi) + \phi \left[ (\rho c_p)_s / (\rho c_p)_f \right] \right]} \cdot \right. \\ & \quad \left. \left[ \frac{k_s + (m-1)k_f - (m-1)\phi(k_f - k_s)}{k_s + (m-1)k_f + \phi(k_f - k_s)} \right] \right\} (1-\phi)^{2.5} b^2 \end{aligned} \right)$$

$$\begin{aligned}
F[10] = \frac{(1-\phi)^{2.5}}{720} & \left[ \begin{aligned} & 2 \left\{ (1-\phi) + \phi \left( \frac{\rho_s}{\rho_f} \right) \right\} \left[ \begin{aligned} & \left( \frac{a(1-\phi)^{2.5}}{15} \right) \left[ \begin{aligned} & 2 \left\{ (1-\phi) + \phi \left( \frac{\rho_s}{\rho_f} \right) \right\} \left[ \begin{aligned} & - \left( \frac{a(1-\phi)^{2.5}}{3} \right) \left\{ (1-\phi) + \phi \left[ (\rho\beta)_s / (\rho\beta)_f \right] \right\} b \\ & + \left( \frac{(1-\phi)^{2.5}}{4} \right) \left\{ (1-\phi) + \phi \left[ (\rho\beta)_s / (\rho\beta)_f \right] \right\}^2 \end{aligned} \right] \\ & - 3 \left\{ (1-\phi) + \phi \left( \frac{\rho_s}{\rho_f} \right) \right\} \left[ \begin{aligned} & - \left( \frac{7a(1-\phi)^{2.5}}{24} \right) \left\{ (1-\phi) + \phi \left[ (\rho\beta)_s / (\rho\beta)_f \right] \right\} b \\ & + \left( \frac{(1-\phi)^5}{6} \right) \left\{ (1-\phi) + \phi \left[ (\rho\beta)_s / (\rho\beta)_f \right] \right\}^2 \end{aligned} \right] \\ & + \left( \frac{\left\{ (1-\phi) + \phi \left[ (\rho\beta)_s / (\rho\beta)_f \right] \right\} Pr}{8} \right) \left[ \begin{aligned} & \frac{1}{\left[ (1-\phi) + \phi \left[ (\rho c_p)_s / (\rho c_p)_f \right] \right]} \\ & \left[ \frac{k_s + (m-1)k_f - (m-1)\phi(k_f - k_s)}{k_s + (m-1)k_f + \phi(k_f - k_s)} \right] \end{aligned} \right] \end{aligned} \right\} ab \\ & - \left( \frac{(1-\phi)^5 \left\{ (1-\phi) + \phi \left[ (\rho\beta)_s / (\rho\beta)_f \right] \right\}}{72} \right) \left\{ (1-\phi) + \phi \left( \frac{\rho_s}{\rho_f} \right) \right\} a^2 b \end{aligned} \right] \\ & - 3 \left\{ (1-\phi) + \phi \left( \frac{\rho_s}{\rho_f} \right) \right\} \left[ \begin{aligned} & \left( \frac{11a(1-\phi)^{2.5}}{105} \right) \left[ \begin{aligned} & 2 \left\{ (1-\phi) + \phi \left( \frac{\rho_s}{\rho_f} \right) \right\} \left[ \begin{aligned} & - \left( \frac{1}{3} \right) (1-\phi)^{2.5} \left\{ (1-\phi) + \phi \left[ (\rho\beta)_s / (\rho\beta)_f \right] \right\} ab \\ & + \left( \frac{1}{4} \right) (1-\phi)^5 \left\{ (1-\phi) + \phi \left[ (\rho\beta)_s / (\rho\beta)_f \right] \right\}^2 \end{aligned} \right] \\ & - 3 \left\{ (1-\phi) + \phi \left( \frac{\rho_s}{\rho_f} \right) \right\} - \left( \frac{7}{24} \right) (1-\phi)^{2.5} \left\{ (1-\phi) + \phi \left[ (\rho\beta)_s / (\rho\beta)_f \right] \right\} ab \\ & + \left( \frac{(1-\phi)^5}{6} \right) \left\{ (1-\phi) + \phi \left[ (\rho\beta)_s / (\rho\beta)_f \right] \right\}^2 \end{aligned} \right] \\ & + \left( \frac{\left\{ (1-\phi) + \phi \left[ (\rho\beta)_s / (\rho\beta)_f \right] \right\} Pr}{8} \right) \left[ \begin{aligned} & \frac{1}{\left[ (1-\phi) + \phi \left[ (\rho c_p)_s / (\rho c_p)_f \right] \right]} \\ & \left[ \frac{k_s + (m-1)k_f - (m-1)\phi(k_f - k_s)}{k_s + (m-1)k_f + \phi(k_f - k_s)} \right] \end{aligned} \right] \end{aligned} \right\} ab \\ & - \left( \frac{(1-\phi)^5}{90} \right) \left\{ (1-\phi) + \phi \left[ (\rho\beta)_s / (\rho\beta)_f \right] \right\} a^2 b \end{aligned} \right] \\ & + \left( \frac{\left\{ (1-\phi) + \phi \left[ (\rho\beta)_s / (\rho\beta)_f \right] \right\} Pr}{14} \right) \left[ \begin{aligned} & \frac{1}{\left[ (1-\phi) + \phi \left[ (\rho c_p)_s / (\rho c_p)_f \right] \right]} \\ & \left[ \frac{k_s + (m-1)k_f - (m-1)\phi(k_f - k_s)}{k_s + (m-1)k_f + \phi(k_f - k_s)} \right] \end{aligned} \right] \left[ \begin{aligned} & - \left( \frac{a^2 Pr}{4} \right) \left[ \begin{aligned} & \frac{1}{\left[ (1-\phi) + \phi \left[ (\rho c_p)_s / (\rho c_p)_f \right] \right]} \\ & \left[ \frac{k_s + (m-1)k_f - (m-1)\phi(k_f - k_s)}{k_s + (m-1)k_f + \phi(k_f - k_s)} \right] \end{aligned} \right] \\ & + \left( \frac{(1-\phi)^{2.5}}{120} \right) \left\{ (1-\phi) + \phi \left( \frac{\rho_s}{\rho_f} \right) \right\} a^2 b \end{aligned} \right] \right] \end{aligned}
\end{aligned}$$

In the same manner, the expressions for  $F[11]$ ,  $F[12]$ ,  $F[13]$ ,  $F[14]$ ,  $F[15]$  are found but they are too large to be included in this paper. Also, using  $p=0, 1, 2, 3...$  in the above recursive relations in Eq. (29), we arrived at following solutions

$$\Theta[2] = 0$$

$$\Theta[3] = 0$$

$$\Theta[4] = -\frac{Pr}{8} \left[ \begin{aligned} & \frac{1}{\left[ (1-\phi) + \phi \left[ (\rho c_p)_s / (\rho c_p)_f \right] \right]} \left[ \frac{k_s + (m-1)k_f - (m-1)\phi(k_f - k_s)}{k_s + (m-1)k_f + \phi(k_f - k_s)} \right] \end{aligned} \right] ab$$

$$\Theta[5] = \frac{Pr}{40} \left\{ \left[ \frac{1}{\left[ (1-\phi) + \phi \left[ (\rho c_p)_s / (\rho c_p)_f \right] \right]} \left[ \frac{k_s + (m-1)k_f - (m-1)\phi(k_f - k_s)}{k_s + (m-1)k_f + \phi(k_f - k_s)} \right] \right] \cdot (1-\phi)^{2.5} \left[ (1-\phi) + \phi \left[ (\rho\beta)_s / (\rho\beta)_f \right] \right] b \right\}$$

$$\Theta[6] = \frac{Pr}{120} \left\{ \left[ \frac{1}{\left[ (1-\phi) + \phi \left[ (\rho c_p)_s / (\rho c_p)_f \right] \right]} \left[ \frac{k_s + (m-1)k_f - (m-1)\phi(k_f - k_s)}{k_s + (m-1)k_f + \phi(k_f - k_s)} \right] \right] \cdot (1-\phi)^{2.5} \left[ (1-\phi) + \phi \left[ (\rho\beta)_s / (\rho\beta)_f \right] \right] b^2 \right\}$$

$$\Theta[7] = -\frac{Pr}{14} \left\{ \left[ \frac{1}{\left[ (1-\phi) + \phi \left[ (\rho c_p)_s / (\rho c_p)_f \right] \right]} \left[ \frac{k_s + (m-1)k_f - (m-1)\phi(k_f - k_s)}{k_s + (m-1)k_f + \phi(k_f - k_s)} \right] \right] \cdot \left[ -\frac{Pr}{4} \left[ \frac{1}{\left[ (1-\phi) + \phi \left[ (\rho c_p)_s / (\rho c_p)_f \right] \right]} \left[ \frac{k_s + (m-1)k_f - (m-1)\phi(k_f - k_s)}{k_s + (m-1)k_f + \phi(k_f - k_s)} \right] \right] a^2 b + \left( \frac{1}{120} \right) (1-\phi)^{2.5} \left[ (1-\phi) + \phi \left[ (\rho)_s / (\rho)_f \right] \right] a^2 b \right] \right\}$$

$$\Theta[8] = -\frac{Pr^2}{128} \left\{ \left[ \frac{1}{\left[ (1-\phi) + \phi \left[ (\rho c_p)_s / (\rho c_p)_f \right] \right]} \left[ \frac{k_s + (m-1)k_f - (m-1)\phi(k_f - k_s)}{k_s + (m-1)k_f + \phi(k_f - k_s)} \right] \right]^2 \cdot (1-\phi)^{2.5} \left[ (1-\phi) + \phi \left[ (\rho\beta)_s / (\rho\beta)_f \right] \right] ab \right\}$$

$$\Theta[9] = \frac{-Pr}{24} \left\{ \left[ \frac{1}{\left[ (1-\phi) + \phi \left[ (\rho c_p)_s / (\rho c_p)_f \right] \right]} \left[ \frac{k_s + (m-1)k_f - (m-1)\phi(k_f - k_s)}{k_s + (m-1)k_f + \phi(k_f - k_s)} \right] \right] \right. \\
\left. \left\{ \frac{Pr}{30} \left\{ \frac{1}{\left[ (1-\phi) + \phi \left[ (\rho c_p)_s / (\rho c_p)_f \right] \right]} \frac{k_s + (m-1)k_f - (m-1)\phi(k_f - k_s)}{k_s + (m-1)k_f + \phi(k_f - k_s)} \right\} \right. \right. \\
\left. \left. \cdot (1-\phi)^{2.5} \left[ (1-\phi) + \phi \left[ (\rho\beta)_s / (\rho\beta)_f \right] \right] ab^2 \right\} \right. \\
\left. - \frac{Pr}{48} \left\{ \left[ \frac{1}{\left[ (1-\phi) + \phi \left[ (\rho c_p)_s / (\rho c_p)_f \right] \right]} \frac{k_s + (m-1)k_f - (m-1)\phi(k_f - k_s)}{k_s + (m-1)k_f + \phi(k_f - k_s)} \right] \right\} \right. \\
\left. \left. \cdot (1-\phi)^5 \left[ (1-\phi) + \phi \left[ (\rho\beta)_s / (\rho\beta)_f \right] \right]^2 b \right\} \right. \\
+ \frac{(1-\phi)^{2.5}}{210} \left( \left( 2 \left[ (1-\phi) + \phi \left[ (\rho)_s / (\rho)_f \right] \right] \left( -\left(\frac{1}{3}\right)(1-\phi)^{2.5} a \left[ (1-\phi) + \phi \left[ (\rho\beta)_s / (\rho\beta)_f \right] \right] b \right) \right. \right. \\
\left. \left. + \left(\frac{1}{4}\right)(1-\phi)^5 \left[ (1-\phi) + \phi \left[ (\rho\beta)_s / (\rho\beta)_f \right] \right]^2 \right) \right. \\
\left. - 3 \left[ (1-\phi) + \phi \left[ (\rho)_s / (\rho)_f \right] \right] \left( -\left(\frac{7}{24}\right)(1-\phi)^{2.5} \left[ (1-\phi) + \phi \left[ (\rho\beta)_s / (\rho\beta)_f \right] \right] ab \right) \right. \\
\left. + \left(\frac{1}{6}\right)(1-\phi)^5 \left[ (1-\phi) + \phi \left[ (\rho\beta)_s / (\rho\beta)_f \right] \right]^2 \right) \right. \\
\left. + \frac{Pr}{8} \left\{ \left[ \frac{1}{\left[ (1-\phi) + \phi \left[ (\rho c_p)_s / (\rho c_p)_f \right] \right]} \right] \left[ \frac{k_s + (m-1)k_f - (m-1)\phi(k_f - k_s)}{k_s + (m-1)k_f + \phi(k_f - k_s)} \right] \right\} \right. \\
\left. \cdot \left[ (1-\phi) + \phi \left[ (\rho\beta)_s / (\rho\beta)_f \right] \right] ab \right\} \right\} b$$

$$\Theta[10] = -\frac{Pr}{4} \left\{ \frac{1}{\left[ \frac{(1-\phi) + \phi \left[ (\rho c_p)_s / (\rho c_p)_f \right]}{k_s + (m-1)k_f - (m-1)\phi(k_f - k_s)} \right]} \right\} \left( -\frac{aPr}{4} \left\{ \frac{1}{\left[ \frac{(1-\phi) + \phi \left[ (\rho c_p)_s / (\rho c_p)_f \right]}{k_s + (m-1)k_f - (m-1)\phi(k_f - k_s)} \right]} \right\} \right. \\ \left. - \frac{Pr}{4} \left\{ \frac{1}{\left[ \frac{(1-\phi) + \phi \left[ (\rho c_p)_s / (\rho c_p)_f \right]}{k_s + (m-1)k_f - (m-1)\phi(k_f - k_s)} \right]} \right\} a^2 b \right. \\ \left. + \left( \frac{1}{120} \right) (1-\phi)^{2.5} \left[ (1-\phi) + \phi \left[ (\rho)_s / (\rho)_f \right] \right] a^2 b \right\} \\ - \frac{3(1-\phi)^5 Pr}{320} \left\{ \frac{1}{\left[ \frac{(1-\phi) + \phi \left[ (\rho c_p)_s / (\rho c_p)_f \right]}{k_s + (m-1)k_f - (m-1)\phi(k_f - k_s)} \right]} \right\} \left[ (1-\phi) + \phi \left[ (\rho\beta)_s / (\rho\beta)_f \right] \right]^2 b^2 \\ - \frac{(1-\phi)^{2.5} a^3 Pr}{120} \left[ (1-\phi) + \phi \left[ (\rho\beta)_s / (\rho\beta)_f \right] \right] \left\{ \frac{1}{\left[ \frac{(1-\phi) + \phi \left[ (\rho c_p)_s / (\rho c_p)_f \right]}{k_s + (m-1)k_f - (m-1)\phi(k_f - k_s)} \right]} \right\} b \\ + \frac{(1-\phi)^{2.5}}{336} \left\{ \left[ (1-\phi) + \phi \left[ (\rho\beta)_s / (\rho\beta)_f \right] \right] \cdot \right. \\ \left. 2 \left\{ \left( \frac{1}{12} \right) a^3 (1-\phi)^{2.5} \left[ (1-\phi) + \phi \left[ (\rho\beta)_s / (\rho\beta)_f \right] \right] \right\} \right. \\ \left. + \left( \frac{1}{6} \right) (1-\phi)^5 \left[ (1-\phi) + \phi \left[ (\rho\beta)_s / (\rho\beta)_f \right] \right]^2 b \right\} \\ - 3 \left\{ \left( \frac{11}{120} \right) a^3 (1-\phi)^{2.5} \left[ (1-\phi) + \phi \left[ (\rho\beta)_s / (\rho\beta)_f \right] \right] \right\} \\ \left. + \left( \frac{1}{8} \right) (1-\phi)^5 \left[ (1-\phi) + \phi \left[ (\rho\beta)_s / (\rho\beta)_f \right] \right]^2 b \right\} b \\ - \frac{Pr}{40} \left\{ \frac{1}{\left[ \frac{(1-\phi) + \phi \left[ (\rho c_p)_s / (\rho c_p)_f \right]}{k_s + (m-1)k_f - (m-1)\phi(k_f - k_s)} \right]} \right\} b \\ \left. \cdot \left[ (1-\phi) + \phi \left[ (\rho\beta)_s / (\rho\beta)_f \right] \right]^2 (1-\phi)^{2.5} \right\}$$

In the same manner, the expressions for  $\Theta[11]$ ,  $\Theta[12]$ ,  $\Theta[13]$ ,  $\Theta[14]$ ,  $\Theta[15]$ ... are found but they are too large to be included in this paper. From the definition in Eq. (17), the solutions of Eqs. (10) and (11) are given as

$$f(\eta) = F[0] + \eta F[1] + \eta^2 F[2] + \eta^3 F[3] + \eta^4 F[4] + \eta^5 F[5] \\ + \eta^6 F[6] + \eta^7 F[7] + \eta^8 F[8] + \eta^9 F[9] + \eta^{10} F[10] + \dots \quad (32)$$

$$\theta(\eta) = \Theta[0] + \eta \Theta[1] + \eta^2 \Theta[2] + \eta^3 \Theta[3] + \eta^4 \Theta[4] + \eta^5 \Theta[5] \\ + \eta^6 \Theta[6] + \eta^7 \Theta[7] + \eta^8 \Theta[8] + \eta^9 \Theta[9] + \eta^{10} \Theta[10] + \dots \quad (33)$$

Now, consider similar fully coupled third and second orders ordinary differential equations presented in Eqs. (9) and (10), but at this time, we take  $a=1$  and  $b=1$



$$g'''(\eta) + (1-\phi)^{2.5} \left\{ \left[ (1-\phi) + \phi \left( \frac{\rho_s}{\rho_f} \right) \right] \left( 3g(\eta)g''(\eta) - 2(f'(\eta))^2 \right) + \left[ (1-\phi) + \phi \left[ (\rho\beta)_s / (\rho\beta)_f \right] \right] \mathcal{G}(\eta) \right\} = 0 \quad (34)$$

$$\mathcal{G}''(\eta) + 3 \left[ \frac{1}{\left[ (1-\phi) + \phi \left[ (\rho C_p)_s / (\rho C_p)_f \right] \right]} \left[ \frac{k_s + (m-1)k_f - (m-1)\phi(k_f - k_s)}{k_s + (m-1)k_f + \phi(k_f - k_s)} \right] \right] Pr_g(\eta) \mathcal{G}'(\eta) = 0 \quad (35)$$

With initial conditions as

$$g = 0, \quad g' = 0, \quad g'' = 1, \quad \mathcal{G} = 1, \quad \mathcal{G}' = 1 \quad \text{when } \eta = 0 \quad (36)$$

Following the similar solution procedures of Eqs. (9) and (10), the solutions of Eqs. (34) and (35) are

$$g(\eta) = G[0] + \eta G[1] + \eta^2 G[2] + \eta^3 G[3] + \eta^4 G[4] + \eta G[5] + \eta^6 G[6] + \eta^7 G[7] + \eta^8 G[8] + \eta^9 G[9] + \eta^{10} G[10] + \dots \quad (37)$$

$$\mathcal{G}(\eta) = \Phi[0] + \eta \Phi[1] + \eta^2 \Phi[2] + \eta^3 \Phi[3] + \eta^4 \Phi[4] + \eta^5 \Phi[5] + \eta^6 \Phi[6] + \eta^7 \Phi[7] + \eta^8 \Phi[8] + \eta^9 \Phi[9] + \eta^{10} \Phi[10] + \dots \quad (38)$$

Where

$$G(0) = 0, \quad G(1) = 0, \quad G(2) = \frac{1}{2}, \quad \theta(0) = 1, \quad \theta(1) = 1$$

$$G[3] = \frac{-(1-\phi)^{2.5}}{6} \left\{ (1-\phi) + \phi \left[ (\rho\beta)_s / (\rho\beta)_f \right] \right\}$$

$$G[4] = \frac{-(1-\phi)^{2.5}}{24} \left\{ (1-\phi) + \phi \left[ (\rho\beta)_s / (\rho\beta)_f \right] \right\}$$

$$G[5] = \frac{(1-\phi)^{2.5}}{120} \left\{ (1-\phi) + \phi \left( \frac{\rho_s}{\rho_f} \right) \right\}$$

$$G[6] = 0$$

$$G[7] = \frac{(1-\phi)^{2.5}}{210} \left( \begin{aligned} & 2 \left\{ (1-\phi) + \phi \left( \frac{\rho_s}{\rho_f} \right) \right\} \left\{ -\left( \frac{1}{3} \right) (1-\phi)^{2.5} \left\{ (1-\phi) + \phi \left[ (\rho\beta)_s / (\rho\beta)_f \right] \right\} \right. \\ & \quad \left. + \left( \frac{1}{4} \right) (1-\phi)^5 \left\{ (1-\phi) + \phi \left[ (\rho\beta)_s / (\rho\beta)_f \right] \right\}^2 \right\} \\ & - 3 \left\{ (1-\phi) + \phi \left( \frac{\rho_s}{\rho_f} \right) \right\} \left\{ \frac{-7(1-\phi)^{2.5}}{24} \left\{ (1-\phi) + \phi \left[ (\rho\beta)_s / (\rho\beta)_f \right] \right\} \right. \\ & \quad \left. + \frac{(1-\phi)^5}{6} \left\{ (1-\phi) + \phi \left[ (\rho\beta)_s / (\rho\beta)_f \right] \right\}^2 \right\} \\ & + \frac{\left\{ (1-\phi) + \phi \left[ (\rho\beta)_s / (\rho\beta)_f \right] \right\} Pr}{8} \left\{ \frac{1}{\left[ (1-\phi) + \phi \left[ (\rho c_p)_s / (\rho c_p)_f \right] \right]} \cdot \right. \\ & \quad \left. \left[ \frac{k_s + (m-1)k_f - (m-1)\phi(k_f - k_s)}{k_s + (m-1)k_f + \phi(k_f - k_s)} \right] \right\} \end{aligned} \right)$$

$$G[8] = \frac{(1-\phi)^{2.5}}{336} \left( \begin{aligned} & 2 \left\{ (1-\phi) + \phi \left( \frac{\rho_s}{\rho_f} \right) \right\} \left\{ \frac{(1-\phi)^{2.5}}{12} \left\{ (1-\phi) + \phi \left( \frac{\rho_s}{\rho_f} \right) \right\} \right. \\ & \quad \left. + \frac{(1-\phi)^5}{6} \left\{ (1-\phi) + \phi \left[ (\rho\beta)_s / (\rho\beta)_f \right] \right\}^2 \right\} \\ & - 3 \left\{ (1-\phi) + \phi \left( \frac{\rho_s}{\rho_f} \right) \right\} \left\{ \frac{11(1-\phi)^{2.5}}{20} \left\{ (1-\phi) + \phi \left( \frac{\rho_s}{\rho_f} \right) \right\} \right. \\ & \quad \left. + \frac{(1-\phi)^5}{8} \left\{ (1-\phi) + \phi \left[ (\rho\beta)_s / (\rho\beta)_f \right] \right\}^2 \right\} \\ & - \left( \frac{\left\{ (1-\phi) + \phi \left[ (\rho\beta)_s / (\rho\beta)_f \right] \right\}^2 Pr (1-\phi)^{2.5}}{40} \right) \left\{ \frac{1}{\left[ (1-\phi) + \phi \left[ (\rho c_p)_s / (\rho c_p)_f \right] \right]} \cdot \right. \\ & \quad \left. \left[ \frac{k_s + (m-1)k_f - (m-1)\phi(k_f - k_s)}{k_s + (m-1)k_f + \phi(k_f - k_s)} \right] \right\} \end{aligned} \right)$$

$$F[9] = \frac{(1-\phi)^{2.5}}{540} \left( \begin{aligned} & 2 \left\{ (1-\phi) + \phi \left( \frac{\rho_s}{\rho_f} \right) \right\} \left\{ -\frac{(1-\phi)^5}{24} \left\{ (1-\phi) + \phi \left[ (\rho\beta)_s / (\rho\beta)_f \right] \right\} \left\{ (1-\phi) + \phi \left( \frac{\rho_s}{\rho_f} \right) \right\} \right. \\ & \quad \left. + \frac{(1-\phi)^5}{36} \left\{ (1-\phi) + \phi \left[ (\rho\beta)_s / (\rho\beta)_f \right] \right\}^2 \right\} \\ & - 3 \left\{ (1-\phi) + \phi \left( \frac{\rho_s}{\rho_f} \right) \right\} \left\{ -\left( \frac{13(1-\phi)^5}{360} \right) \left\{ (1-\phi) + \phi \left[ (\rho\beta)_s / (\rho\beta)_f \right] \right\} \left\{ (1-\phi) + \phi \left( \frac{\rho_s}{\rho_f} \right) \right\} \right. \\ & \quad \left. + \left( \frac{(1-\phi)^5}{48} \right) \left\{ (1-\phi) + \phi \left[ (\rho\beta)_s / (\rho\beta)_f \right] \right\}^2 \right\} \\ & - \left( \frac{\left\{ (1-\phi) + \phi \left[ (\rho\beta)_s / (\rho\beta)_f \right] \right\}^2}{240} \right) Pr \left\{ \frac{1}{\left[ (1-\phi) + \phi \left[ (\rho c_p)_s / (\rho c_p)_f \right] \right]} \cdot \right. \\ & \quad \left. \left[ \frac{k_s + (m-1)k_f - (m-1)\phi(k_f - k_s)}{k_s + (m-1)k_f + \phi(k_f - k_s)} \right] \right\} (1-\phi)^{2.5} \end{aligned} \right)$$

$$G[10] = \frac{(1-\phi)^{2.5}}{720} \left[ \begin{aligned} & 2 \left\{ (1-\phi) + \phi \left( \frac{\rho_s}{\rho_f} \right) \right\} \left[ \begin{aligned} & \left( \frac{(1-\phi)^{2.5}}{15} \right) \left[ \begin{aligned} & 2 \left\{ (1-\phi) + \phi \left( \frac{\rho_s}{\rho_f} \right) \right\} \left[ \begin{aligned} & - \left( \frac{a(1-\phi)^{2.5}}{3} \right) \left\{ (1-\phi) + \phi \left[ (\rho\beta)_s / (\rho\beta)_f \right] \right\} \\ & + \left( \frac{(1-\phi)^{2.5}}{4} \right) \left\{ (1-\phi) + \phi \left[ (\rho\beta)_s / (\rho\beta)_f \right] \right\}^2 \end{aligned} \right] \\ & - 3 \left\{ (1-\phi) + \phi \left( \frac{\rho_s}{\rho_f} \right) \right\} \left[ \begin{aligned} & - \left( \frac{7a(1-\phi)^{2.5}}{24} \right) \left\{ (1-\phi) + \phi \left[ (\rho\beta)_s / (\rho\beta)_f \right] \right\} \\ & + \left( \frac{(1-\phi)^5}{6} \right) \left\{ (1-\phi) + \phi \left[ (\rho\beta)_s / (\rho\beta)_f \right] \right\}^2 \end{aligned} \right] \\ & + \left( \frac{\left\{ (1-\phi) + \phi \left[ (\rho\beta)_s / (\rho\beta)_f \right] \right\} Pr}{8} \right) \left[ \begin{aligned} & \frac{1}{\left[ (1-\phi) + \phi \left[ (\rho c_p)_s / (\rho c_p)_f \right] \right]} \\ & \cdot \left[ \frac{k_s + (m-1)k_f - (m-1)\phi(k_f - k_s)}{k_s + (m-1)k_f + \phi(k_f - k_s)} \right] \end{aligned} \right] \end{aligned} \right] \\ & - \left( \frac{(1-\phi)^5 \left\{ (1-\phi) + \phi \left[ (\rho\beta)_s / (\rho\beta)_f \right] \right\}}{72} \right) \left\{ (1-\phi) + \phi \left( \frac{\rho_s}{\rho_f} \right) \right\} \end{aligned} \right] \\ & - 3 \left\{ (1-\phi) + \phi \left( \frac{\rho_s}{\rho_f} \right) \right\} \left[ \begin{aligned} & \left( \frac{11(1-\phi)^{2.5}}{105} \right) \left[ \begin{aligned} & 2 \left\{ (1-\phi) + \phi \left( \frac{\rho_s}{\rho_f} \right) \right\} \left[ \begin{aligned} & - \left( \frac{1}{3} \right) (1-\phi)^{2.5} \left\{ (1-\phi) + \phi \left[ (\rho\beta)_s / (\rho\beta)_f \right] \right\} \\ & + \left( \frac{1}{4} \right) (1-\phi)^5 \left\{ (1-\phi) + \phi \left[ (\rho\beta)_s / (\rho\beta)_f \right] \right\}^2 \end{aligned} \right] \\ & - 3 \left\{ (1-\phi) + \phi \left( \frac{\rho_s}{\rho_f} \right) \right\} \left[ \begin{aligned} & - \left( \frac{7}{24} \right) (1-\phi)^{2.5} \left\{ (1-\phi) + \phi \left[ (\rho\beta)_s / (\rho\beta)_f \right] \right\} \\ & + \left( \frac{(1-\phi)^5}{6} \right) \left\{ (1-\phi) + \phi \left[ (\rho\beta)_s / (\rho\beta)_f \right] \right\}^2 \end{aligned} \right] \\ & + \left( \frac{\left\{ (1-\phi) + \phi \left[ (\rho\beta)_s / (\rho\beta)_f \right] \right\} Pr}{8} \right) \left[ \begin{aligned} & \frac{1}{\left[ (1-\phi) + \phi \left[ (\rho c_p)_s / (\rho c_p)_f \right] \right]} \\ & \cdot \left[ \frac{k_s + (m-1)k_f - (m-1)\phi(k_f - k_s)}{k_s + (m-1)k_f + \phi(k_f - k_s)} \right] \end{aligned} \right] \end{aligned} \right] \\ & - \left( \frac{(1-\phi)^5}{90} \right) \left\{ (1-\phi) + \phi \left[ (\rho\beta)_s / (\rho\beta)_f \right] \right\} \end{aligned} \right] \\ & + \left( \frac{\left\{ (1-\phi) + \phi \left[ (\rho\beta)_s / (\rho\beta)_f \right] \right\} Pr}{14} \right) \left[ \begin{aligned} & \frac{1}{\left[ (1-\phi) + \phi \left[ (\rho c_p)_s / (\rho c_p)_f \right] \right]} \\ & \cdot \left[ \frac{k_s + (m-1)k_f - (m-1)\phi(k_f - k_s)}{k_s + (m-1)k_f + \phi(k_f - k_s)} \right] \end{aligned} \right] \\ & + \left( \frac{Pr}{4} \right) \left[ \begin{aligned} & \frac{1}{\left[ (1-\phi) + \phi \left[ (\rho c_p)_s / (\rho c_p)_f \right] \right]} \\ & \cdot \left[ \frac{k_s + (m-1)k_f - (m-1)\phi(k_f - k_s)}{k_s + (m-1)k_f + \phi(k_f - k_s)} \right] \end{aligned} \right] \\ & + \left( \frac{(1-\phi)^{2.5}}{120} \right) \left\{ (1-\phi) + \phi \left( \frac{\rho_s}{\rho_f} \right) \right\} \end{aligned} \right] \end{aligned} \right]$$

$$\Phi[2] = 0$$

$$\Phi[3] = 0$$

$$\Phi[4] = -\frac{Pr}{8} \left\{ \frac{1}{\left[ (1-\phi) + \phi \left[ (\rho c_p)_s / (\rho c_p)_f \right] \right]} \left[ \frac{k_s + (m-1)k_f - (m-1)\phi(k_f - k_s)}{k_s + (m-1)k_f + \phi(k_f - k_s)} \right] \right\}$$

$$\Phi[5] = \frac{Pr}{40} \left\{ \left[ \frac{1}{\left[ (1-\phi) + \phi \left[ (\rho c_p)_s / (\rho c_p)_f \right] \right]} \left[ \frac{k_s + (m-1)k_f - (m-1)\phi(k_f - k_s)}{k_s + (m-1)k_f + \phi(k_f - k_s)} \right] \right] \cdot (1-\phi)^{2.5} \left[ (1-\phi) + \phi \left[ (\rho\beta)_s / (\rho\beta)_f \right] \right] \right\}$$

$$\begin{aligned}
\Phi[6] &= \frac{Pr}{120} \left\{ \left\{ \frac{1}{\left[ (1-\phi) + \phi \left[ (\rho c_p)_s / (\rho c_p)_f \right] \right]} \left[ \frac{k_s + (m-1)k_f - (m-1)\phi(k_f - k_s)}{k_s + (m-1)k_f + \phi(k_f - k_s)} \right] \right\} \right. \\
&\quad \left. \cdot (1-\phi)^{2.5} \left[ (1-\phi) + \phi \left[ (\rho\beta)_s / (\rho\beta)_f \right] \right] \right\} \\
\Phi[7] &= -\frac{Pr}{14} \left\{ \left\{ \frac{1}{\left[ (1-\phi) + \phi \left[ (\rho c_p)_s / (\rho c_p)_f \right] \right]} \left[ \frac{k_s + (m-1)k_f - (m-1)\phi(k_f - k_s)}{k_s + (m-1)k_f + \phi(k_f - k_s)} \right] \right\} \right. \\
&\quad \left. - \frac{Pr}{4} \left\{ \frac{1}{\left[ (1-\phi) + \phi \left[ (\rho c_p)_s / (\rho c_p)_f \right] \right]} \left[ \frac{k_s + (m-1)k_f - (m-1)\phi(k_f - k_s)}{k_s + (m-1)k_f + \phi(k_f - k_s)} \right] \right\} \right. \\
&\quad \left. + \left( \frac{1}{120} \right) (1-\phi)^{2.5} \left[ (1-\phi) + \phi \left[ (\rho)_s / (\rho)_f \right] \right] \right\} \\
\Phi[8] &= -\frac{Pr^2}{128} \left\{ \left\{ \frac{1}{\left[ (1-\phi) + \phi \left[ (\rho c_p)_s / (\rho c_p)_f \right] \right]} \left[ \frac{k_s + (m-1)k_f - (m-1)\phi(k_f - k_s)}{k_s + (m-1)k_f + \phi(k_f - k_s)} \right] \right\}^2 \right. \\
&\quad \left. \cdot (1-\phi)^{2.5} \left[ (1-\phi) + \phi \left[ (\rho\beta)_s / (\rho\beta)_f \right] \right] \right\} \\
\Phi[9] &= -\frac{Pr}{24} \left\{ \left\{ \frac{1}{\left[ (1-\phi) + \phi \left[ (\rho c_p)_s / (\rho c_p)_f \right] \right]} \left[ \frac{k_s + (m-1)k_f - (m-1)\phi(k_f - k_s)}{k_s + (m-1)k_f + \phi(k_f - k_s)} \right] \right\} \right. \\
&\quad \left\{ \frac{Pr}{30} \left\{ \frac{1}{\left[ (1-\phi) + \phi \left[ (\rho c_p)_s / (\rho c_p)_f \right] \right]} \frac{k_s + (m-1)k_f - (m-1)\phi(k_f - k_s)}{k_s + (m-1)k_f + \phi(k_f - k_s)} \right\} \right. \\
&\quad \left. \cdot (1-\phi)^{2.5} \left[ (1-\phi) + \phi \left[ (\rho\beta)_s / (\rho\beta)_f \right] \right] \right\} \\
&\quad - \frac{Pr}{48} \left\{ \left\{ \frac{1}{\left[ (1-\phi) + \phi \left[ (\rho c_p)_s / (\rho c_p)_f \right] \right]} \frac{k_s + (m-1)k_f - (m-1)\phi(k_f - k_s)}{k_s + (m-1)k_f + \phi(k_f - k_s)} \right\} \right. \\
&\quad \left. \cdot (1-\phi)^5 \left[ (1-\phi) + \phi \left[ (\rho\beta)_s / (\rho\beta)_f \right] \right]^2 \right\} \\
&\quad + \frac{(1-\phi)^{2.5}}{210} \left[ 2 \left[ (1-\phi) + \phi \left[ (\rho)_s / (\rho)_f \right] \right] \left( -\left( \frac{1}{3} \right) (1-\phi)^{2.5} \left[ (1-\phi) + \phi \left[ (\rho\beta)_s / (\rho\beta)_f \right] \right] \right) \right. \\
&\quad \left. + \left( \frac{1}{4} \right) (1-\phi)^5 \left[ (1-\phi) + \phi \left[ (\rho\beta)_s / (\rho\beta)_f \right] \right]^2 \right] \\
&\quad - 3 \left[ (1-\phi) + \phi \left[ (\rho)_s / (\rho)_f \right] \right] \left( -\left( \frac{7}{24} \right) (1-\phi)^{2.5} \left[ (1-\phi) + \phi \left[ (\rho\beta)_s / (\rho\beta)_f \right] \right] \right. \\
&\quad \left. + \left( \frac{1}{6} \right) (1-\phi)^5 \left[ (1-\phi) + \phi \left[ (\rho\beta)_s / (\rho\beta)_f \right] \right]^2 \right) \\
&\quad + \frac{Pr}{8} \left\{ \left\{ \frac{1}{\left[ (1-\phi) + \phi \left[ (\rho c_p)_s / (\rho c_p)_f \right] \right]} \right\} \cdot \left[ \frac{k_s + (m-1)k_f - (m-1)\phi(k_f - k_s)}{k_s + (m-1)k_f + \phi(k_f - k_s)} \right] \right\} \\
&\quad \left. \cdot \left[ (1-\phi) + \phi \left[ (\rho\beta)_s / (\rho\beta)_f \right] \right] \right\} \right\}
\end{aligned}$$

$$\Phi[10] = -\frac{Pr}{4} \left\{ \left[ \frac{1}{\left[ \frac{(1-\phi) + \phi \left[ (\rho c_p)_s / (\rho c_p)_f \right]}{k_s + (m-1)k_f - (m-1)\phi(k_f - k_s)} \right]} \right] \right. \\ \left. - \frac{Pr}{4} \left\{ \left[ \frac{1}{\left[ \frac{(1-\phi) + \phi \left[ (\rho c_p)_s / (\rho c_p)_f \right]}{k_s + (m-1)k_f - (m-1)\phi(k_f - k_s)} \right]} \right] \right. \right. \\ \left. \left. + \left( \frac{1}{120} \right) (1-\phi)^{2.5} \left[ (1-\phi) + \phi \left[ (\rho)_s / (\rho)_f \right] \right] \right\} \right. \\ \left. - \frac{3(1-\phi)^5 Pr}{320} \left[ \frac{1}{\left[ \frac{(1-\phi) + \phi \left[ (\rho c_p)_s / (\rho c_p)_f \right]}{k_s + (m-1)k_f - (m-1)\phi(k_f - k_s)} \right]} \right] \left[ (1-\phi) + \phi \left[ (\rho\beta)_s / (\rho\beta)_f \right] \right]^2 \right. \\ \left. - \frac{(1-\phi)^{2.5} Pr}{120} \left[ (1-\phi) + \phi \left[ (\rho\beta)_s / (\rho\beta)_f \right] \right] \left\{ \left[ \frac{1}{\left[ \frac{(1-\phi) + \phi \left[ (\rho c_p)_s / (\rho c_p)_f \right]}{k_s + (m-1)k_f - (m-1)\phi(k_f - k_s)} \right]} \right] \right. \right. \\ \left. \left. + \frac{(1-\phi)^{2.5}}{336} \left\{ \left[ \frac{(1-\phi) + \phi \left[ (\rho\beta)_s / (\rho\beta)_f \right]}{\left( \left( \frac{11}{120} \right) (1-\phi)^{2.5} \left[ (1-\phi) + \phi \left[ (\rho\beta)_s / (\rho\beta)_f \right] \right] \right]} \right. \right. \right. \right. \\ \left. \left. \left. + \left( \frac{1}{8} \right) (1-\phi)^5 \left[ (1-\phi) + \phi \left[ (\rho\beta)_s / (\rho\beta)_f \right] \right]^2 \right\} \right\} \right. \\ \left. - \frac{Pr}{40} \left\{ \left[ \frac{1}{\left[ \frac{(1-\phi) + \phi \left[ (\rho c_p)_s / (\rho c_p)_f \right]}{k_s + (m-1)k_f - (m-1)\phi(k_f - k_s)} \right]} \right] \right. \right. \\ \left. \left. \cdot \left[ (1-\phi) + \phi \left[ (\rho\beta)_s / (\rho\beta)_f \right] \right]^2 (1-\phi)^{2.5} \right\} \right\} \right\}$$

The functions in Eq. (32) and (33) and that in Eq. (37) and (38) have relations as follows:

$$f(\eta) = a^k g(a^q \eta) \rightarrow f'(\eta) = a^{k+q} g'(a^q \eta) \rightarrow f'(\infty) = a^{k+q} g'(\infty)$$

and

$$\theta(\eta) = b^r \mathcal{G}(b^s \eta) \rightarrow \theta(\infty) = b^r \mathcal{G}(\infty)$$

From Eq. (11),  $f'(\infty) = 0$  and  $\theta(\infty) = 0$ . Since  $a \neq 0$  and  $b \neq 0 \rightarrow g'(\infty) = 0$  and  $\mathcal{G}(\infty) = 0$ .

## 5 Applying Multi-Step DTM

To solve the boundary layer problems, the domain  $[0, \infty)$  is replaced by  $[0, \eta_\infty]$ . But  $\eta_\infty$  should be great enough that the solution is not dependent on. The solution domain should be divided to  $N$  equal parts ( $H = \eta_\infty / N$ ). So, we have

$$g_i'''(\eta_i) + (1-\phi)^{2.5} \left\{ \left[ (1-\phi) + \phi \left( \frac{\rho_s}{\rho_f} \right) \right] \left( 3g_i(\eta_i) g_i''(\eta_i) - 2(f_i'(\eta_i))^2 \right) \right. \\ \left. + \left[ (1-\phi) + \phi \left[ (\rho\beta)_s / (\rho\beta)_f \right] \right] \mathcal{G}_i(\eta_i) \right\} = 0 \quad (39)$$

$$(i-1)H \leq \eta_i < iH, \quad \text{for } i \leq i \leq N$$

$$\mathcal{G}_i''(\eta_i) + 3 \left\{ \frac{1}{\left[ (1-\phi) + \phi \left[ (\rho C_p)_s / (\rho C_p)_f \right] \right]} \left[ \frac{k_s + (m-1)k_f - (m-1)\phi(k_f - k_s)}{k_s + (m-1)k_f + \phi(k_f - k_s)} \right] \right. \\ \left. Pr g_i(\eta_i) \mathcal{G}_i'(\eta_i) \right\} = 0 \quad (40)$$

Applying multi-step DTM on Eq. (39) and Eq. (40)

$$G_i(p+3) = \frac{(1-\phi)^{2.5} H^3}{(p+1)(p+2)(p+3)} \left\{ \left[ (1-\phi) + \phi \left( \frac{\rho_s}{\rho_f} \right) \right] \left[ 2 \sum_{l=0}^p \frac{(l+1)}{H} G_i(l+1) \frac{(p-l+1)}{H} G_i(p-l+1) \right. \right. \\ \left. \left. - 3 \sum_{l=0}^p G_i(l) \frac{(p-l+1)(p-l+2)}{H^2} G_i(p-l+2) \right] \right. \\ \left. - \left[ (1-\phi) + \phi \left[ (\rho\beta)_s / (\rho\beta)_f \right] \right] \mathcal{G}_i(p) \right\} \quad (41) \\ \text{for } i \leq i \leq N$$

$$\mathcal{G}_i(p+2) = \frac{-3H^2 Pr}{(p+1)(p+2)} \left\{ \left[ \frac{1}{\left[ (1-\phi) + \phi \left[ (\rho C_p)_s / (\rho C_p)_f \right] \right]} \left[ \frac{k_s + (m-1)k_f - (m-1)\phi(k_f - k_s)}{k_s + (m-1)k_f + \phi(k_f - k_s)} \right] \right] \right. \\ \left. \times \sum_{l=0}^p \frac{(l+1)}{H} \mathcal{G}_i(l+1) G_i(p-l) \right\} \quad (42) \\ \text{for } i \leq i \leq N$$

The initial conditions for the problem are considered for the first sub domain ( $i=1$ ). Following Eq. (23), the differential transform for the initial conditions for Eq. (34) and (35) and for Eqs. (41) and (42) are

$$G_1(0) = g_1(0) = 0, \quad G_1(1) = H g_1'(0) = 0, \quad G_1(2) = \frac{H^2}{2} g_1'' = \frac{H^2}{2}, \quad (43)$$

$$\Psi_1(0) = \mathcal{G}_1(0) = 1, \quad \Psi_1(1) = H \mathcal{G}_1'(0) = H$$

The boundary conditions of each subdomain are continuity of the

$$g_i(\eta_i), \quad g_i'(\eta_i), \quad g_i''(\eta_i), \quad \mathcal{G}_i(\eta_i), \quad \text{and} \quad \mathcal{G}_i'(\eta_i) \quad (44)$$

These boundary conditions can be obtained from Eq. (25):

$$g_i(\eta_i), \quad g_i'(\eta_i), \quad g_i''(\eta_i), \quad \mathcal{G}_i(\eta_i), \quad \text{and} \quad \mathcal{G}_i'(\eta_i) \quad (44)$$

$$g_i(\eta_{i+1}) = \sum_{k=0}^m G_i(k) \quad (45a)$$

$$g_{i+1}(\eta_{i+1}) = G_{i+1}(0) \rightarrow G_{i+1}(0) = \sum_{k=0}^m G_i(k)$$

$$g'_i(\eta_{i+1}) = \sum_{k=1}^m \frac{k}{H} G_i(k) \quad (45b)$$

$$g'_i(\eta_{i+1}) = \frac{G_{i+1}(1)}{H} \rightarrow G_{i+1}(1) = \sum_{k=1}^m k G_i(k)$$

$$g''_i(\eta_{i+1}) = \sum_{k=2}^m \frac{k(k-1)}{H^2} G_i(k) \quad (45c)$$

$$g''_i(\eta_{i+1}) = \frac{2G_{i+1}(2)}{H^2} \rightarrow G_{i+1}(2) = \frac{1}{2} \sum_{k=1}^m k(k-1) G_i(k)$$

$$\mathcal{G}_i(\eta_{i+1}) = \sum_{k=0}^m \Psi_i(k) \quad (46a)$$

$$\mathcal{G}_{i+1}(\eta_{i+1}) = \Psi_{i+1}(0) \rightarrow \Psi_{i+1}(0) = \sum_{k=0}^m \Psi_i(k)$$

$$\mathcal{G}'_i(\eta_{i+1}) = \sum_{k=1}^m \frac{k}{H} \Psi_i(k) \quad (46b)$$

$$\mathcal{G}'_i(\eta_{i+1}) = \frac{\Psi_{i+1}(1)}{H} \rightarrow \Psi_{i+1}(1) = \sum_{k=1}^m k \Psi_i(k)$$

The values of the  $g'(\eta_\infty)$  and  $\mathcal{G}(\eta_\infty)$  can be calculated by differentiating from Eq. (24)

$$g'_i(\infty) \simeq g'_i(\eta_\infty) = g'_i(\eta_{N+1}) = \sum_{k=1}^m \frac{k}{H} G_N(k) \quad (47)$$

$$\mathcal{G}_i(\infty) \simeq \mathcal{G}_i(\eta_\infty) = \mathcal{G}_i(\eta_{N+1}) = \sum_{k=0}^m \Psi_N(k)$$

Now, Eq. (9) and (10) are solved with a similar process like Eqs. (34) and (35) using multi-step DTM. The only difference is that the condition  $f''(0) = a$  is replaced by the condition  $g''(0) = 1$ . It should be noted as mentioned previously that the unknown parameters “ $a$ ” and “ $b$ ” in the solutions are unknown constants. The infinite boundary conditions i.e.  $\eta \rightarrow \infty$ ,  $f' = 0$ ,  $\theta = 0$  are applied. The resulting simultaneous equations are solved to obtain the values of  $a$  and  $b$  for the respective values of the physical and thermal properties of the nanofluids under considerations.

## 6 Flow and heat transfer parameters

In addition to the determination of the velocity and temperature distributions, it is often desirable to compute other physically important quantities (such as shear stress, drag, heat

transfer rate and heat transfer coefficient) associated with the free convection flow and heat transfer problem. Consequently, two parameters, a flow parameter and a heat transfer parameter, are computed. The local heat transfer coefficient at the surface of the vertical plate can be obtained from

### 6.1 Fluid flow parameter

Skin friction coefficient

$$c_f = \frac{\tau_w}{\rho_{nf} u^2} = \frac{\mu_{nf} \left. \frac{\partial u}{\partial y} \right|_{y=0}}{\rho_{nf} u^2} = \frac{\mu_{nf} \left( \frac{\partial u}{\partial \eta} \cdot \frac{\partial \eta}{\partial y} \right) \Big|_{y=0}}{\rho_{nf} u^2} \quad (48)$$

After the dimensionless exercise,

$$c_f (Re_x)^{1/2} = \frac{f''(0)}{(1-\phi)^{2.5}} \quad (49)$$

$$c_f (Re_x)^{1/2} \frac{\tau_w}{(4Gr_x^3)^{1/4} (\nu\mu)} = f''(0) \frac{f''(0)}{(1-\phi)^{2.5}}$$

### 6.2 Heat transfer parameter

$$h_x = -\frac{k_{nf}}{T_w - T_\infty} \left( \frac{\partial T}{\partial y} \right)_{y=0} = -k_{nf} \theta'(0) \frac{1}{x} \left( \frac{1}{4} Gr_x \right)^{1/4} \quad (50)$$

### 6.3 The local Nusselt number

The local Nusselt number is

$$Nu_x = \frac{h_x x}{k_{nf}} = -\left( \frac{x}{T_w - T_\infty} \right) \left( \frac{\partial T}{\partial y} \right)_{y=0} = -\theta'(0) \left( \frac{1}{4} Gr_x \right)^{1/4} \quad (51)$$

$$Nu_x = -\frac{\theta'(0)}{\sqrt{2}} Gr_x^{1/4} = f((Pr) Gr_x^{1/4})$$

Where  $\phi(Pr) = -\frac{\theta'(0)}{\sqrt{2}}$  is a function of Prandtl number. The dependence of  $\phi$  on the Prandtl number is evidenced by Eq. (51). It could also be shown that

$$\frac{Nu_x}{(Re_x)^{1/2}} = -\frac{k_{nf}}{k_f} \theta'(0) = -\left[ \frac{k_s + (m-1)k_f - (m-1)\phi(k_f - k_s)}{k_s + (m-1)k_f + \phi(k_f - k_s)} \right] \theta'(0) \quad (52)$$

Where  $Re_x$  and  $Gr_x$  are the local Reynold and Grashof numbers defined as:

$$Re_x = \frac{ux}{\nu_{nf}} \quad \text{and} \quad Gr_x = \frac{g\beta(T_w - T_\infty)x^3}{\nu^3}$$



## 7 Results and Discussion

Tables (5-22) present various comparisons of results of the present study and the past works for viscous fluid i.e. when the volume fraction of the nanoparticle is zero ( $\phi=0$ ). It could be seen from the Tables that there are excellent agreements between the past results and the present study. Moreover, the Tables present the effects of Prandtl number on the flow and heat transfer processes.

**Table 5** Comparison of results for the skin friction parameter

$f''(0)$					
Pr	Sparrow & Gregg [5]	Kuiken[8]	Present study	Residue on [5]	Residue on [8]
0.003	1.0223	1.0151	1.0224	0.0001	0.0073
0.008	0.9955	0.9801	0.9955	0.0000	0.0154
0.020	0.9590	0.9284	0.9591	0.0001	0.0307
0.030	0.9384	0.8966	0.9384	0.0000	0.0418

**Table 6** Comparison of results of  $f(\infty)$

$f(\infty)$					
Pr	Sparrow & Gregg [5]	Kuiken[8]	Present study	Residue on [5]	Residue on [8]
0.003	8.7060	8.8763	8.7061	0.0001	0.1702
0.008	5.4018	5.4152	5.4018	0.0000	0.0134
0.020	3.4093	3.4055	3.4093	0.0000	0.0038
0.030	2.7878	2.7710	2.7878	0.0000	0.0168

**Table 7** Comparison of results of  $-\theta'(0)$

$Nu_x / (G_x Pr^2)^{\frac{1}{4}} = -\theta'(0)$					
Pr	Sparrow & Gregg [5]	Kuiken[8]	Present study	Residue on [5]	Residue on [8]
0.003	8.7060	8.8763	8.7061	0.0001	0.1702
0.003	0.5827	0.5827	0.5827	0.0000	0.0000
0.008	0.5729	0.5714	0.5728	0.0001	0.0014
0.020	0.5582	0.5546	0.5582	0.0000	0.0036
0.030	0.5497	0.5443	0.5497	0.0000	0.0054

**Table 8** Comparison of results of  $f(\eta)$ ,  $f'(\eta)$  and  $f''(\eta)$  at  $Pr=0.01$

	$f(\eta)$		$f'(\eta)$		$f''(\eta)$	
$\eta$	Ostrach[2]	Present study	Ostrach[2]	Present study	Ostrach[2]	Present study
0.0	0.0000	0.0000	0.0000	0.0000	0.9862	0.9845
1.0	0.3376	0.3376	0.5379	0.5379	0.1734	0.1734
2.0	0.9023	0.9023	0.5535	0.5535	0.0641	0.0641
3.0	1.4200	1.4200	0.4810	0.4810	0.0719	0.0719
4.0	1.8665	1.8665	0.4136	0.4136	0.0629	0.0629
5.0	2.2501	2.2501	0.3548	0.3548	0.0549	0.0549
6.0	2.5787	2.5787	0.3035	0.3035	0.0479	0.0479
7.0	2.8593	2.8593	0.2586	0.2586	0.0419	0.0419
9.0	3.2999	3.2999	0.1853	0.1853	0.0319	0.0319
11	3.6123	3.6123	0.1297	0.1297	0.0241	0.0241
13	3.8276	3.8276	0.0877	0.0877	0.0181	0.0181
16	4.0204	4.0204	0.0441	0.0441	0.0114	0.0114
20	4.1226	4.1226	0.0108	0.0108	0.0057	0.0057

22	4.1343	4.1343	0.0015	0.0015	0.0037	0.0037
----	--------	--------	--------	--------	--------	--------

**Table 9** Comparison of results of  $f(\eta)$ ,  $f'(\eta)$  and  $f''(\eta)$  at  $Pr=1$

$\eta$	$f(\eta)$		$f'(\eta)$		$f''(\eta)$	
	Ostrach [2]	Present study	Ostrach [2]	Present study	Ostrach [2]	Present study
0.0	0.0000	0.0000	0.0000	0.0000	0.6421	0.6421
1.0	0.1809	0.1809	0.2502	0.2502	-0.0263	-0.0263
2.0	0.3859	0.3859	0.1450	0.1450	-0.1233	-0.1233
3.0	0.4791	0.4791	0.0524	0.0524	-0.0602	-0.0602
4.0	0.5096	0.5096	0.0151	0.0151	-0.0202	-0.0202
5.0	0.5177	0.5177	0.0035	0.0035	-0.0057	-0.0057
6.0	0.5194	0.5194	0.0004	0.0004	-0.0014	-0.0014

**Table 10** Comparison of results of  $f(\eta)$ ,  $f'(\eta)$  and  $f''(\eta)$  at  $Pr=2$

$\eta$	$f(\eta)$		$f'(\eta)$		$f''(\eta)$	
	Ostrach[2]	Present study	Ostrach[2]	Present study	Ostrach[2]	Present study
0.0	0.0000	0.0000	0.0000	0.0000	0.5713	0.5712
1.0	0.1508	0.1508	0.1994	0.1994	-0.0440	-0.0440
2.0	0.3066	0.3066	0.1050	0.1050	-0.0960	-0.0960
3.0	0.3731	0.3731	0.0373	0.0373	-0.0416	-0.0416
4.0	0.3953	0.3953	0.0018	0.0018	-0.0138	-0.0138
5.0	0.4023	0.4023	0.0037	0.0037	-0.0042	-0.0042
7.0	0.4053	0.4053	0.0005	0.0005	-0.0004	-0.0004
8.0	0.4056	0.4056	0.0002	0.0002	-0.0001	-0.0001
9.0	0.4058	0.4058	0.0001	0.0001	0.0000	0.0000
10.0	0.4059	0.4059	0.0001	0.0001	0.0000	0.0000
11.0	0.4059	0.4059	0.0001	0.0001	0.0000	0.0000

**Table 11** Comparison of results of  $f(\eta)$ ,  $f'(\eta)$  and  $f''(\eta)$  at  $Pr=10$

$\eta$	$f(\eta)$		$f'(\eta)$		$f''(\eta)$	
	Ostrach[2]	Present study	Ostrach[2]	Present study	Ostrach[2]	Present study
0.0	0.0000	0.0000	0.0000	0.0000	0.4192	0.4191
1.0	0.0908	0.0908	0.1066	0.1066	-0.0462	-0.0462
2.0	0.1714	0.1714	0.0567	0.0567	-0.0400	-0.0400
3.0	0.2119	0.2119	0.0276	0.0276	-0.0201	-0.0201
4.0	0.2314	0.2314	0.0132	0.0132	-0.0098	-0.0098
5.0	0.2408	0.2408	0.0063	0.0063	-0.0047	-0.0047
7.0	0.2474	0.2474	0.0014	0.0014	-0.0011	-0.0011
8.0	0.2484	0.2484	0.0007	0.0007	-0.0005	-0.0005
9.0	0.2489	0.2489	0.0003	0.0003	-0.0002	-0.0002
10.0	0.2491	0.2491	0.0002	0.0002	-0.0001	-0.0001

**Table 12** Comparison of results of  $f(\eta)$ ,  $f'(\eta)$  and  $f''(\eta)$  at  $Pr=100$

$\eta$	$f(\eta)$		$f'(\eta)$		$f''(\eta)$	
	Ostrach[2]	Present study	Ostrach[2]	Present study	Ostrach[2]	Present study
0.0	0.0000	0.0000	0.0000	0.0000	0.2517	0.2517
1.0	0.0371	0.0371	0.0385	0.0385	-0.0140	-0.0140
2.0	0.0692	0.0692	0.0265	0.0265	-0.0101	-0.0101
3.0	0.0912	0.0912	0.0180	0.0180	-0.0071	-0.0071
4.0	0.1061	0.1061	0.0121	0.0121	-0.0049	-0.0049
6.0	0.1226	0.1226	0.0053	0.0053	-0.0022	-0.0022
8.0	0.1297	0.1297	0.0022	0.0022	-0.0010	-0.0010
9.0	0.1315	0.1315	0.0014	0.0014	-0.0007	-0.0007
10.0	0.1326	0.1326	0.0008	0.0008	-0.0005	-0.0005
11.0	0.1332	0.1332	0.0004	0.0004	-0.0003	-0.0003

12.0	0.1335	0.1335	0.0002	0.0002	-0.0002	-0.0002
13.0	0.1336	0.1335	0.0000	0.0000	-0.0001	-0.0001
<b>Table 13</b> Comparison of results of $f(\eta)$ , $f'(\eta)$ and $f''(\eta)$ at $Pr=1000$						
$\eta$	$f(\eta)$		$f'(\eta)$		$f''(\eta)$	
	Ostrach[2]	Present study	Ostrach[2]	Present study	Ostrach[2]	Present study
0.0	0.0000	0.0000	0.0000	0.0000	0.1450	0.1450
1.0	0.0135	0.0135	0.0136	0.0136	-0.0027	-0.0027
3.0	0.0358	0.0358	0.0090	0.0090	-0.0019	-0.0019
5.0	0.0912	0.0912	0.0180	0.0180	-0.0071	-0.0071
7.0	0.0603	0.0603	0.0039	0.0039	-0.0008	-0.0008
8.0	0.0638	0.0638	0.0032	0.0032	-0.0007	-0.0007
10.0	0.0691	0.0691	0.0022	0.0022	-0.0004	-0.0004
12.0	0.0727	0.0727	0.0015	0.0015	-0.0003	-0.0003
14.0	0.0752	0.0752	0.0011	0.0011	-0.0002	-0.0002
16.0	0.0771	0.0771	0.0008	0.0008	-0.0001	-0.0001
18.0	0.0786	0.0786	0.0007	0.0007	0.0000	0.0000
20.0	0.0798	0.0798	0.0006	0.0006	0.0000	0.0000
22.0	0.0809	0.0809	0.0005	0.0005	0.0000	0.0000

**Table 14** Comparison of results of  $\theta(\eta)$ , and  $\theta'(\eta)$  at  $Pr=0.01$ 

$\eta$	$\theta(\eta)$		$\theta'(\eta)$	
	Ostrach[2]	Present	Ostrach[2]	Present
0.0	1.0000	1.0000	-0.0812	-0.0812
1.0	0.9189	0.9189	-0.0809	-0.0809
2.0	0.8387	0.8387	-0.0794	-0.0794
3.0	0.7606	0.7606	-0.0766	-0.0766
4.0	0.6857	0.6857	-0.0720	-0.0720
5.0	0.6149	0.6149	-0.0686	-0.0686
6.0	0.5487	0.5487	-0.0638	-0.0638
7.0	0.4874	0.4874	-0.0588	-0.0588
9.0	0.3799	0.3799	-0.0489	-0.0489
11	0.2915	0.2915	-0.0397	-0.0397
13	0.2202	0.2202	-0.0317	-0.0317
16	0.1399	0.1399	-0.0223	-0.0223
20	0.0894	0.0894	-0.0137	-0.0137
21	0.0565	0.0565	-0.0121	-0.0121
22	0.0452	0.0452	-0.0107	-0.0107

**Table 15** Comparison of results of  $\theta(\eta)$ , and  $\theta'(\eta)$  at  $Pr=1$ 

$\eta$	$\theta(\eta)$		$\theta'(\eta)$	
	Ostrach[2]	Present study	Ostrach[2]	Present study
0.0	1.0000	1.0000	-0.5671	-0.5671
1.0	0.4638	0.4638	-0.4589	-0.4589
2.0	0.1422	0.1422	-0.1907	-0.1907
3.0	0.0339	0.0339	-0.0509	-0.0509
4.0	0.0072	0.0072	-0.0115	-0.0115
5.0	0.0014	0.0014	-0.0024	-0.0024
6.0	0.0002	0.0002	-0.0005	-0.0005

**Table 16** Comparison of results of  $\theta(\eta)$ , and  $\theta'(\eta)$  at  $Pr=2$ 

$\eta$	$\theta(\eta)$		$\theta'(\eta)$	
	Ostrach[2]	Present study	Ostrach[2]	Present study
0.0	1.0000	1.0000	-0.7165	-0.7165
1.0	0.3476	0.3476	-0.5002	-0.5002
2.0	0.0592	0.0592	-0.1207	-0.1207
3.0	0.0066	0.0066	-0.0152	-0.0152
4.0	0.0007	0.0007	-0.0015	-0.0015
5.0	0.0001	0.0001	-0.0686	-0.0686
6.0	0.5487	0.5487	-0.0001	-0.0001
7.0	0.0000	0.0000	0.0000	0.0000
8.0	0.0000	0.0000	0.0000	0.0000
9.0	0.0000	0.0000	0.0000	0.0000
10	0.0000	0.0000	0.0000	0.0000

**Table 17** Comparison of results of  $\theta(\eta)$ , and  $\theta'(\eta)$  at  $Pr=10$ 

$\eta$	$\theta(\eta)$		$\theta'(\eta)$	
	Ostrach[2]	Present study	Ostrach[2]	Present study
0.0	1.0000	1.0000	-1.1694	-1.1694
1.0	0.1090	0.1090	-0.3753	-0.3753
2.0	0.0012	0.0012	-0.0065	-0.0065
3.0	0.0000	0.0000	0.0000	0.0000
4.0	0.0000	0.0000	0.0000	0.0000
5.0	0.0000	0.0000	0.0000	0.0000
7.0	0.0000	0.0000	0.0000	0.0000
8.0	0.0000	0.0000	0.0000	0.0000
9.0	0.0000	0.0000	0.0000	0.0000
10	0.0000	0.0000	0.0000	0.0000

**Table 18** Comparison of results of  $\theta(\eta)$ , and  $\theta'(\eta)$  at  $Pr=100$ 

$\eta$	$\theta(\eta)$		$\theta'(\eta)$	
	Ostrach[2]	Present study	Ostrach[2]	Present study
0.0	1.0000	1.0000	-2.1910	-2.1910
1.0	0.0012	0.0012	-0.0149	-0.0149
2.0	0.0000	0.0000	0.0000	0.0000
3.0	0.0000	0.0000	0.0000	0.0000
4.0	0.0000	0.0000	0.0000	0.0000
7.0	0.0000	0.0000	0.0000	0.0000
8.0	0.0000	0.0000	0.0000	0.0000
9.0	0.0000	0.0000	0.0000	0.0000
10	0.0000	0.0000	0.0000	0.0000
11	0.0000	0.0000	0.0000	0.0000
12	0.0000	0.0000	0.0000	0.0000
13	0.0000	0.0000	0.0000	0.0000

<b>Table 19</b> Comparison of results of $\theta(\eta)$ , and $\theta'(\eta)$ at $Pr=1000$				
	$\theta(\eta)$		$\theta'(\eta)$	
$\eta$	Ostrach [2]	Present study	Ostrach [2]	Present study
0.0	1.0000	1.0000	-3.9660	-3.9660
1.0	0.0000	0.0000	0.0000	0.0000
2.6	0.0000	0.0000	0.0000	0.0000
3.0	0.0000	0.0000	0.0000	0.0000
5.0	0.0000	0.0000	0.0000	0.0000
5.8	0.0000	0.0000	0.0000	0.0000
7.0	0.0000	0.0000	0.0000	0.0000
8.0	0.0000	0.0000	0.0000	0.0000
10	0.0000	0.0000	0.0000	0.0000
20	0.0000	0.0000	0.0000	0.0000
22	0.0000	0.0000	0.0000	0.0000
23	0.0000	0.0000	0.0000	0.0000

**Table 20** Comparison of results of  $f''(\eta)$  and  $\theta'(\eta)$  at different Prandtl numbers

$Pr$	Kuo[22]		Na and Hibb[12]		Present study	
	$f''(0)$	$\theta'(0)$	$f''(0)$	$\theta'(0)$	$f''(0)$	$\theta'(0)$
0.72	0.6760	-0.5046	0.6760	-0.5046	0.6760	-0.5046
0.60	0.6947	-0.4721	0.6946	-0.4725	0.6947	-0.4721
0.50	0.7132	-0.4411	0.7131	-0.4420	0.7132	-0.4411
0.40	0.7356	-0.4053	0.7354	-0.4066	0.7356	-0.4053
0.30	0.7636	-0.3623	0.7633	-0.3641	0.7636	-0.3623
0.20	0.8015	-0.3078	0.8009	-0.3101	0.8015	-0.3078
0.10	0.8600	-0.2298	0.8590	-0.2326	0.8600	-0.2298
0.06	0.8974	-0.1834	0.8961	-0.1864	0.8974	-0.1834
0.04	0.9233	-0.1526	0.9221	-0.1556	0.9233	-0.1526
0.01	0.9845	-0.0832	0.9887	-0.0817	0.9885	-0.0832
1.00	0.6421	-0.5671	0.6421	-0.5671	0.6421	-0.5671
1.10	0.6323	-0.5862	0.6323	-0.5860	0.6323	-0.5862
1.20	0.6233	-0.6040	0.6234	-0.6036	0.6233	-0.6040
1.30	0.6151	-0.6208	0.6152	-0.6202	0.6151	-0.6208
1.40	0.6075	-0.6365	0.6076	-0.6358	0.6075	-0.6365
1.50	0.6005	-0.6515	0.6006	-0.6506	0.6005	-0.6515
1.60	0.5939	-0.6656	0.5940	-0.6646	0.5939	-0.6656
1.70	0.5877	-0.6792	0.5879	-0.6780	0.5877	-0.6792
1.80	0.5819	-0.6921	0.5821	-0.6908	0.5819	-0.6921
1.90	0.5764	-0.7045	0.5767	-0.7031	0.5764	-0.7045
2.00	0.5712	-0.7164	0.5715	-0.7149	0.5712	-0.7164
2.00	0.5712	-0.7164	0.5713	-0.7165	0.5712	-0.7164
3.00	0.5308	-0.8154	0.5312	-0.8145	0.5308	-0.8154
4.00	0.5029	-0.8914	0.5036	-0.8898	0.5029	-0.8914
5.00	0.4817	-0.9539	0.4827	-0.9517	0.4817	-0.9539
6.00	0.4648	-1.0073	0.4660	-1.0047	0.4648	-1.0073
7.00	0.4507	-1.0542	0.4522	-1.0512	0.4507	-1.0542
8.00	0.4387	-1.0961	0.4405	-1.0930	0.4387	-1.0961
9.00	0.4283	-1.1342	0.4304	-1.1309	0.4283	-1.1342
10.00	0.4191	-1.1692	0.4215	-1.1658	0.4191	-1.1692

**Table 21** Comparison of results of  $f''(\eta)$  at different Prandtl number

$f''(0)$			
Pr	Kuiken [34]	Mosta [17]	Present study
0.001	1.12313813	1.12313813	1.12313813
0.01	1.06338086	1.06338086	1.06338086
0.1	0.92408304	0.92408304	0.92408304
1	0.69321163	0.69321163	0.69321163
10	0.44711652	0.44711652	0.44711652
100	0.26452354	0.26452354	0.26452354
1000	0.15129020	0.15129020	0.15129020
10000	0.08554085	0.08554085	0.08554085

**Table 22** Comparison of results of  $f''(\eta)$  at different Prandtl number

$-\theta'(0)$				
Pr	Kuiken [34]	Mosta et al. [17]	Mosta et al. [17]	Present study
0.001	0.04680746	0.04680746	0.04680746	0.04680746
0.01	0.13576074	0.13576074	0.13576074	0.13576074
0.1	0.35005967	0.35005967	0.35005967	0.35005967
1	0.76986120	0.76986120	0.76986119	0.76986121
10	1.49709921	1.49709921	1.49709921	1.49709921
100	2.74688550	2.74688550	2.74688549	2.74688550
1000	4.93494763	4.93494763	4.93494756	4.93494762
10000	8.80444927	8.80444927	8.80444960	8.80444958

Although, the nonlinear partial differential equations are the same in all aspects to the present problems under investigation, there are slight differences between the transformed nonlinear ordinary differential equations in Mosta et al. [17] of Eq. (7) and developed Eq. (12) and (13) in this present study (where the volume-fraction of the nanoparticle is set to zero) due to the differences in the adopted similarity variables. It is shown that using the multi-DTM as applied in this work to the transformed nonlinear ordinary differential equations in Mosta et al. [17], excellent agreements are recorded between the results of the present study and that of Mosta et al. [17] and Kuiken [34] as shown in Tables (17) and (18).

The variations of nanoparticle volume fraction with dynamic viscosity and thermal conductivity ratios of Copper (II) Oxide-water nanofluid are shown in Fig (2) and (3), respectively. Also, Fig. (3) show the effects of nanoparticle shape on thermal conductivity ratio. It is depicted in the figure that the thermal conductivity of nanofluid varies linearly and increases with increase in nanoparticle volume fraction. It is also observed that the suspensions of particles with high shape factor or low sphericity have higher thermal conductivity ratio of the nanofluid. With spherical shape nanoparticle have the lowest thermal conductivity ratio and lamina shape nanoparticle have the highest thermal conductivity ratio. The effects of the flow and heat transfer controlling parameters on the velocity and temperature distributions are shown in Figs. (4–17) for different shapes, type and volume-fraction of nanoparticles at Prandtl number of 0.01-1000.

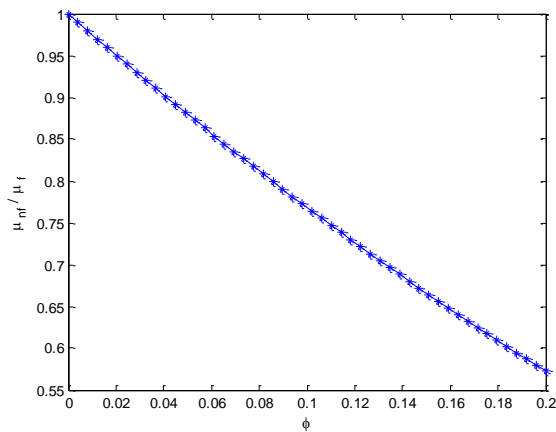


**Figure 2** Variation of nanofluid dynamic viscosity ratio with nanoparticle volume fraction

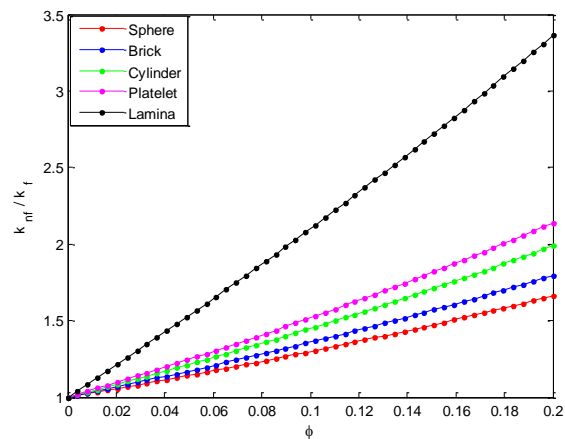


**Figure 3** Effects of nanoparticle shape on thermal conductivity ratio of nanofluid

### 7.1 Effect of nanoparticle volume fraction on nanofluid velocity and temperature distributions for different values of Prandtl number

Figs. (4-7) show the effects nanoparticle concentration/volume fraction and Prandtl number on velocity and temperature profiles Copper (II) Oxide-water nanofluid. It is indicated in the Figures that as the volume-fraction or concentration of the nanoparticle in the nanofluid increases, the velocity decreases. However, an opposite trend in the temperature profile is observed i.e. the nanofluid temperature increases as the volume-fraction of the nanoparticles in the basefluid increases. This is because, the solid volume fraction has significant impacts on the thermal conductivity.

The increased volume fraction of nanoparticles in basefluid results in higher thermal conductivity of the basefluid which increases the heat enhancement capacity of the basefluid. Also, one of the possible reasons for the enhancement on heat transfer of nanofluids can be explained by the high concentration of nanoparticles in the thermal boundary layer at the wall side through the migration of nanoparticles. It should also be stated that the thickness of thermal boundary layer rises with increasing the values of nanoparticle volume fraction. This consequently reduces the velocity of the nanofluid as the shear stress and skin friction are increased. The figures also show the effects of Prandtl number (Pr) on the velocity and temperature profiles. It is indicated that the velocity of the nanofluid decreases as the Pr increases but the temperature of the nanofluid increases as the Pr increases.

This is because the nanofluid with higher Prandtl number has a relatively low thermal conductivity, which reduces conduction, and thereby reduces the thermal boundary-layer thickness, and as a consequence, increases the heat transfer rate at the surface. For the case of the fluid velocity that decreases with the increase of Pr, the reason is that fluid of the higher Prandtl number means more viscous fluid, which increases the boundary-layer thickness and thus, reduces the shear stress and consequently, retards the flow of the nanofluid.

Also, it can be seen that the velocity distribution for small value of Prandtl number consist of two distinct regions. A thin region near the wall of the plate where there are large velocity gradients due to viscous effects and a region where the velocity gradients are small compared with those near the wall. In the later region, the viscous effects are negligible and the flow of fluid in the region can be considered to be inviscid.

Also, such region tends to create uniform accelerated flow at the surface of the plate.

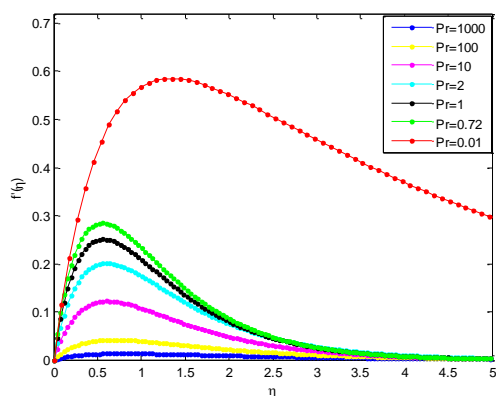


**Figure 4a** Effects of Prandtl number on the velocity profile when  $\phi=0.020$

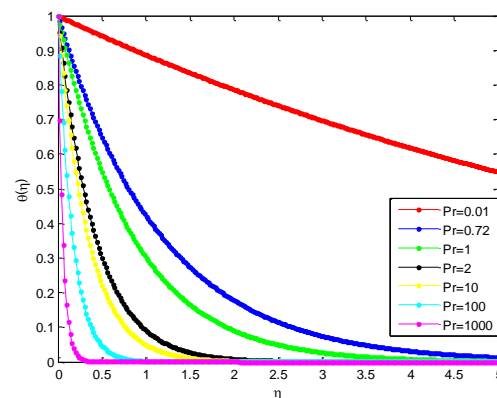


**Figure 4b** Effects of Prandtl number on temperature profile when  $\phi=0.020$

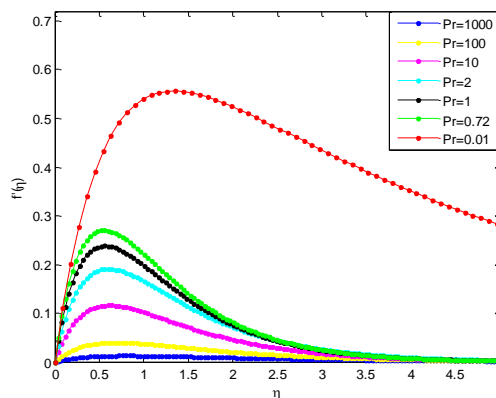


**Figure 5a** Effects of Prandtl number on the velocity profile when  $\phi=0.040$

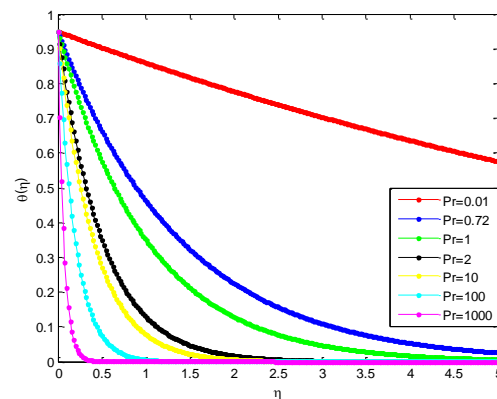


**Figure 5b** Effects of Prandtl number on temperature profile when  $\phi=0.040$

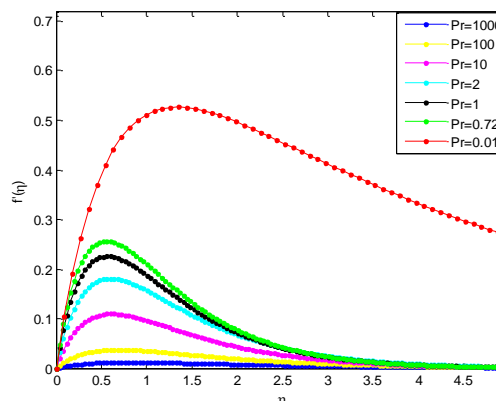


**Figure 6a** Effects of Prandtl number on the velocity profile when  $\phi=0.060$

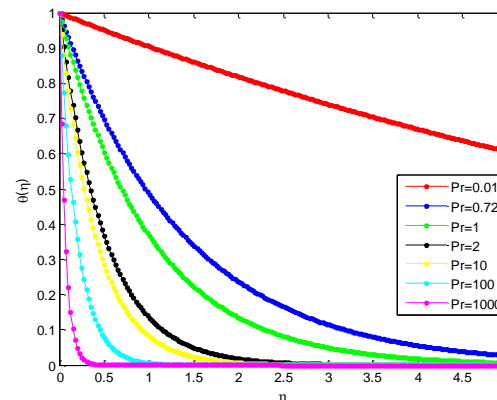


**Figure 6b** Effects of Prandtl number on temperature profile when  $\phi=0.060$



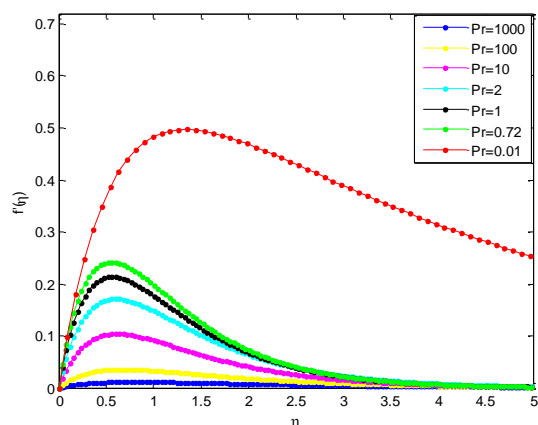


**Figure 7a** Effects of Prandtl number on the velocity profile when  $\phi=0.080$

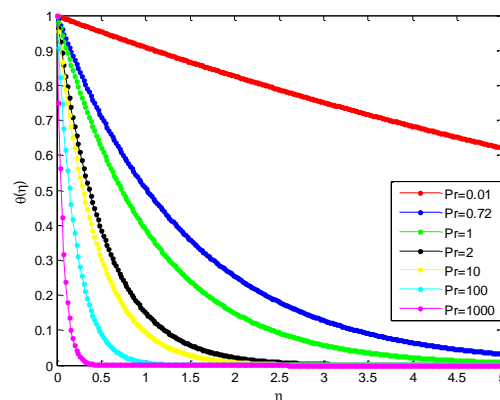


**Figure 7b** Effects of Prandtl number on temperature profile when  $\phi=0.080$

The use of nanoparticles in the fluids exhibited better properties relating to the heat transfer of fluid than heat transfer enhancement through the use of suspended millimeter- or micrometer-sized particles which potentially cause some severe problems, such as abrasion, clogging, high pressure drop, and sedimentation of particles. The very low concentrations applications and nanometer sizes properties of nanoparticles in base fluid prevent the sedimentation in the flow that may clog the channel. It should be added that the theoretical prediction of enhanced thermal conductivity of the base fluid and prevention of clogging, abrasion, high pressure drop and sedimentation through the addition of nanoparticles in base fluid have been supported with experimental evidences in literature.

## 7.2 Effect of nanoparticle shape on nanofluid velocity and temperature distributions for different values of Prandtl number

It has observed experimentally that the nanoparticle shape have significant impacts on the thermal conductivity. Therefore, the effects of nanoparticle shape at different values of Prandtl number on velocity and temperature profiles of Copper (II) Oxide-water nanofluid are shown in Fig. (8-13). It is indicated that the maximum decrease in velocity and maximum increase in temperature are caused by lamina, platelets, cylinder, bricks and sphere, respectively.

It is observed that lamina shaped nanoparticle carries maximum velocity whereas spherical shaped nanoparticle has better enhancement on heat transfer than other nanoparticle shapes.

In fact, it is in accordance with the physical expectation since it is well known that the lamina nanoparticle has greater shape factor than other nanoparticles of different shapes, therefore, the lamina nanoparticle comparatively gains maximum temperature than others. The velocity decreases is maximum in spherical nanoparticles when compared with other shapes. The enhancement observed at lower volume fractions for non-spherical particles is attributed to the percolation chain formation, which perturbs the boundary layer and thereby increases the local Nusselt number values.

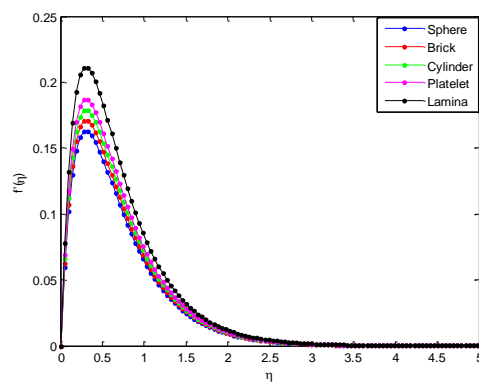


**Figure 8a** Effect of nanoparticle shape on velocity distribution of the nanofluid

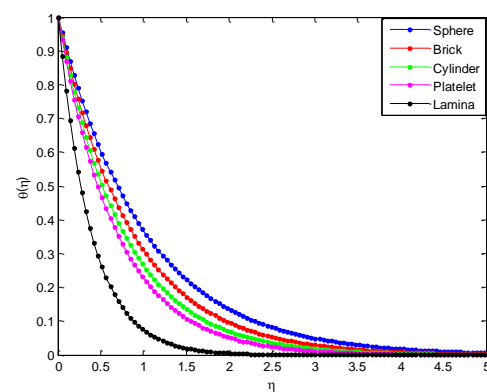


**Figure 8b** Effects of nanoparticle shape on temperature distribution of nanofluid

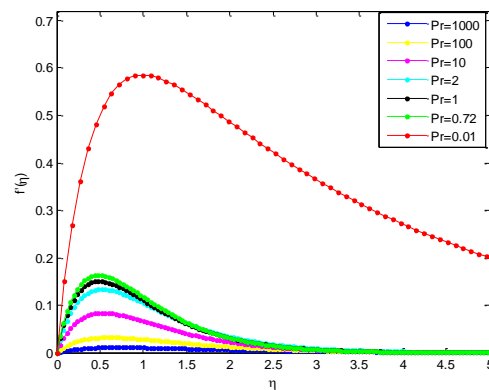


**Figure 9a** Effects of Prandtl number on velocity profile for spherical shape nanoparticle

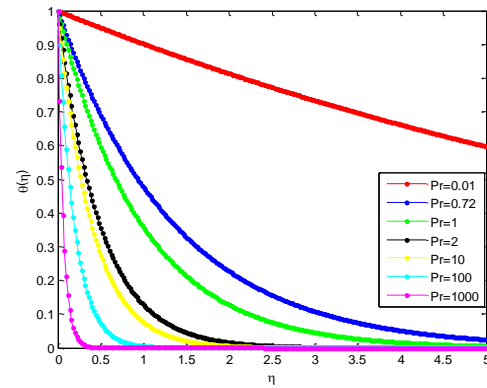


**Figure 9b** Effects of Prandtl number on temperature profile for spherical shape nanoparticle

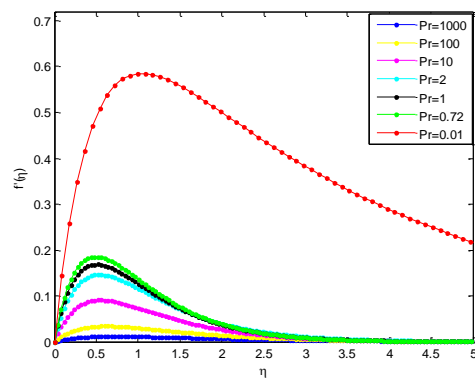


**Figure 10a** Effects of Prandtl number on velocity profile for brick shape nanoparticle

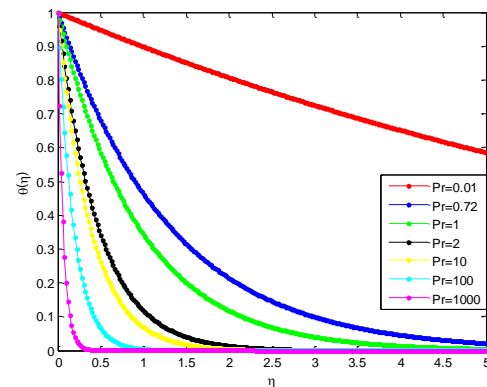


**Figure 10b** Effects of Prandtl number on temperature profile for brick shape nanoparticle

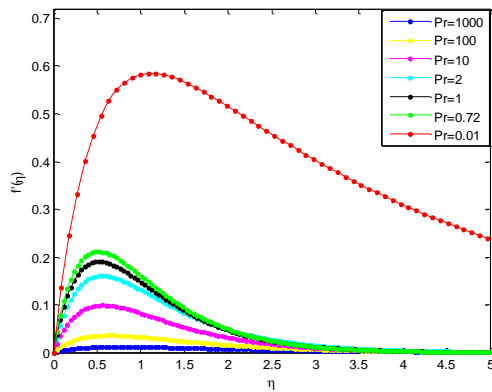


**Figure 11a** Effects of Prandtl number on velocity profile for cylindrical shape nanoparticle

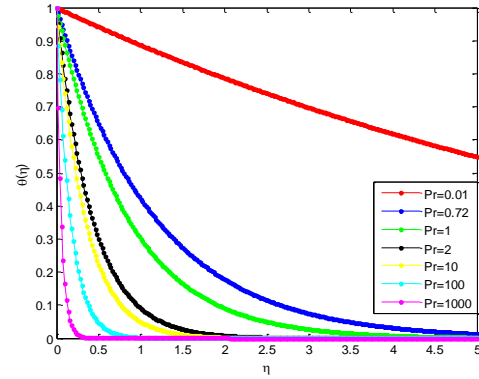


**Figure 11b** Effects of Prandtl number on temperature profile for cylindrical shape nanoparticle

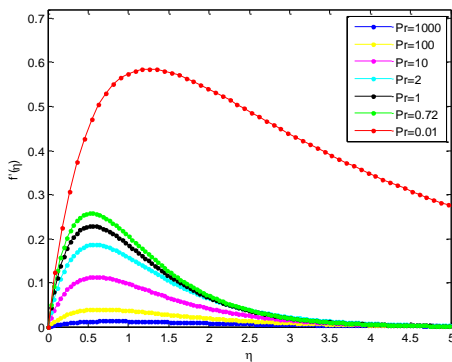


**Figure 12a** Effects of Prandtl number on velocity profile for platelet shape nanoparticle

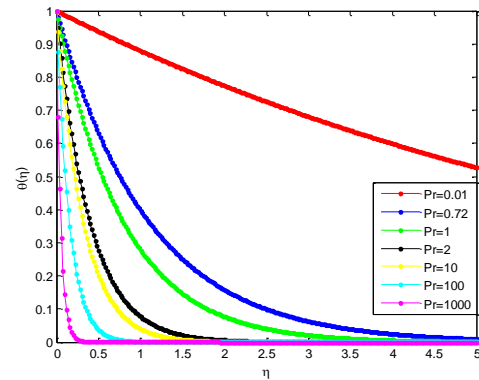


**Figure 12b** Effects of Prandtl number on temperature profile for platelet shape nanoparticle

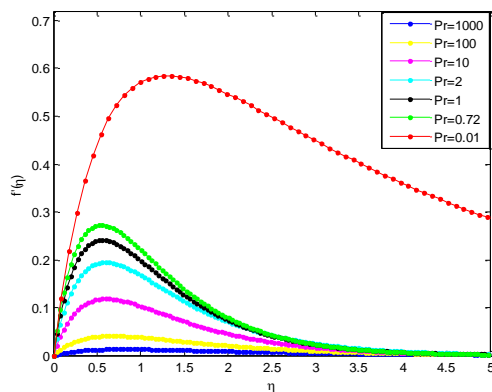


**Figure 13a** Effects of Prandtl number on velocity profile for lamina shape nanoparticle

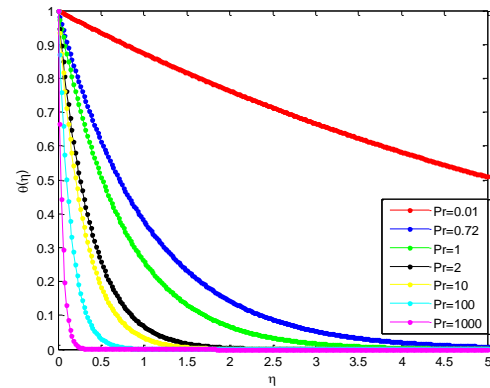


**Figure 13b** Effects of Prandtl number on temperature profile for lamina shape nanoparticle

It is evident from this study that proper choice of nanoparticles will be helpful in controlling velocity and heat transfer. It is also observed that irreversibility process can be reduced by using nanoparticles, especially the spherical particles. This can potentially result in higher enhancement in the thermal conductivity of a nanofluid containing elongated particles compared to the one containing spherical nanoparticle, as exhibited by the experimental data in the literature.

### 7.3 Effect of type of nanoparticle on nanofluid velocity and temperature distribution for different values of Prandtl number

The variations of the velocity and temperature profiles against  $\eta$  for various types of nanoparticles ( $\text{TiO}_2$ ,  $\text{CuO}$ ,  $\text{Al}_2\text{O}_3$  and SWCNTs) are shown in Fig. (14-17). Using a common basefluid for all the nanoparticle types, it is observed that the maximum decrease in velocity and maximum increase in temperature are caused by  $\text{TiO}_2$ ,  $\text{CuO}$ ,  $\text{Al}_2\text{O}_3$  and SWCNTs, respectively. It is observed that SWCNTs nanoparticle carries maximum decreases velocity but has better enhancement on heat transfer than other nanoparticle shapes.

In accordance with the physical expectation well, the SWCNTs nanoparticle has higher thermal conductivity than other types of nanoparticles, therefore, the SWCNTs nanoparticle comparatively gains maximum temperature than others. The increased thermal conductivity of the base fluid due to the use of nanoparticle of higher thermal conductivity increases the heat enhancement capacity of the base fluid. Also, it is observed that the velocity decreases is maximum in SWCNTs nanoparticles when compared with other type of nanoparticles.

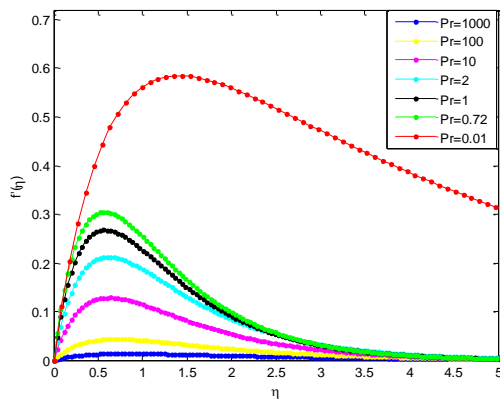


**Figure 14a** Effects of Prandtl number on velocity profile for  $\text{TiO}_2$  nanoparticle

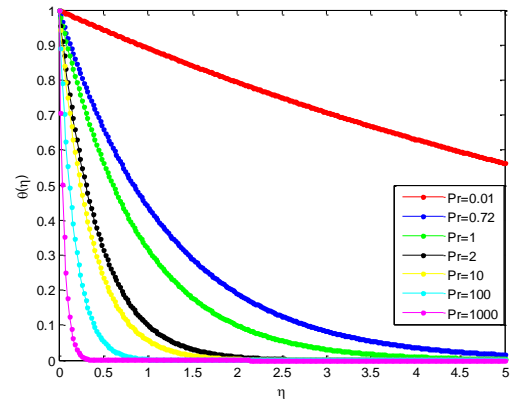


**Figure 14b** Effects of Prandtl number on temperature profile for  $\text{TiO}_2$  nanoparticle

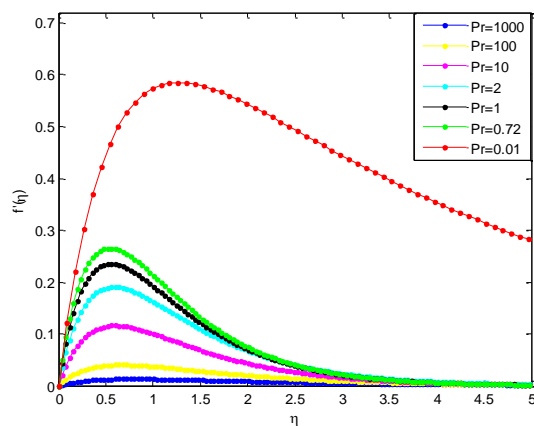


**Figure 15a** Effects of Prandtl number on velocity profile for  $\text{CuO}$  nanoparticle

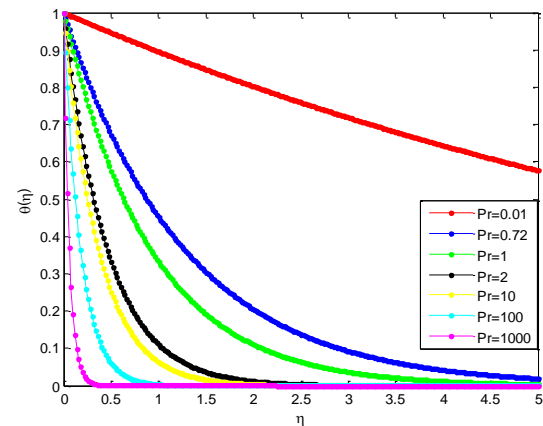


**Figure 15b** Effects of Prandtl number on temperature profile for  $\text{CuO}$  nanoparticle

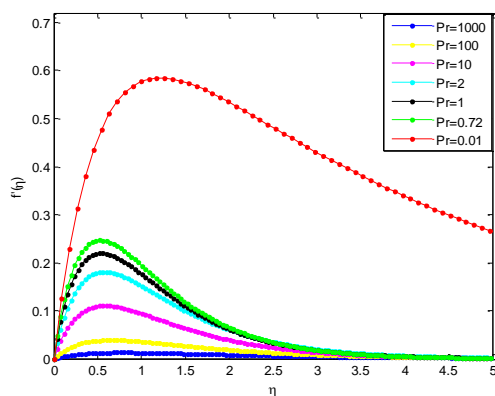


**Figure 16a** Effects of Prandtl number on velocity profile for  $\text{Al}_2\text{O}_3$  nanoparticle

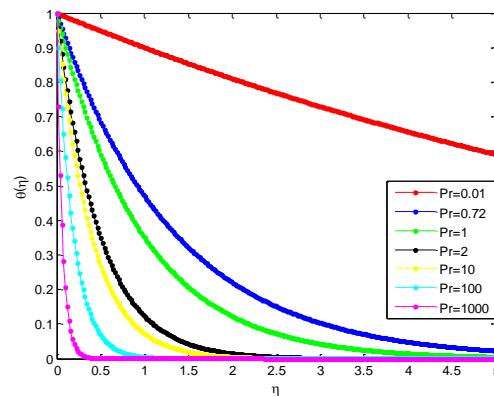


**Figure 16b** Effects of Prandtl number on temperature profile for  $\text{Al}_2\text{O}_3$  nanoparticle

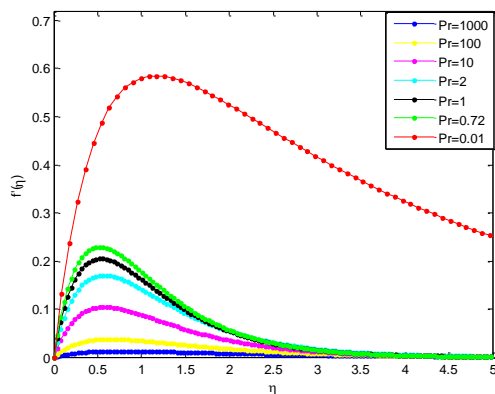


**Figure 17a** Effects of Prandtl number on velocity profile for SWCNTs nanoparticle

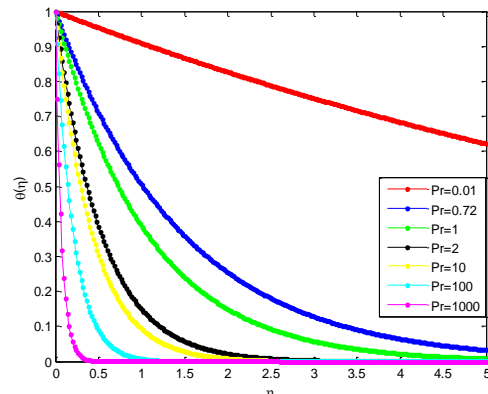


**Figure 17b** Effects of Prandtl number on temperature profile for SWCNTs nanoparticle

This is because, the solid thermal conductivity has significant impacts on the momentum boundary layer of the nanofluid. The thickness of the momentum boundary layer increases with the increase in thermal conductivity. It is observed that the thickness of the thermal boundary layer enhances in presence of higher thermal conductivity nanoparticle.

Therefore, the sensitivity of the boundary layer thickness to the type of nanoparticle is correlated to the value of the thermal conductivity of the nanoparticle used which consequently leads to enhancement of thermal conductivity of the nanofluid.

## Conclusion

In this work, free convection boundary layer flow and heat transfer of nanofluids of different shapes nano-size particles over a vertical plate at very low and high values of Prandtl number have been analyzed. The governing systems of nonlinear partial differential equations of the flow and heat transfer processes are transformed to system of nonlinear ordinary differential equation through similarity variables. The systems of fully coupled nonlinear ordinary differential equations have been solved using multi-step differential transformation method. The accuracies of the developed analytical solutions were verified with the results generated by some other methods as presented in the past works.

The developed analytical solutions were used to investigate the effects of Prandtl number, nanoparticles size and shapes on the flow and heat transfer behaviour of various nanofluids. From the parametric studies, the following observations were established.

- i. The velocity of the nanofluid decreases as the Prandtl number increases but the temperature of the nanofluid increases as the Prandtl number increases.
- ii. The velocity of the nanofluid decreases as the volume-fraction or concentration of the nanoparticle in the basefluid increases. However, an opposite trend or behaviour in the temperature profile was observed which showed that as the nanofluid temperature increases as the volume-fraction of the nanoparticles in the basefluid increases.
- iii. The lamina shaped nanoparticle carries maximum velocity whereas spherical shaped nanoparticle has better enhancement on heat transfer than other nanoparticle shapes. The maximum decrease in velocity and maximum increase in temperature are caused by lamina shaped nanoparticle and followed by platelets, cylinder, bricks and sphere shaped nanoparticles, respectively.
- iv. Using a common basefluid to all the nanoparticle types considered in this work, it was observed that SWCNTs nanoparticle carries maximum decrease in velocity but has better enhancement on heat transfer than other nanoparticle shapes. Also, it was observed that the maximum decrease in velocity and maximum increase in temperature are caused by  $\text{TiO}_2$  and followed by  $\text{CuO}$ ,  $\text{Al}_2\text{O}_3$  and SWCNTs nanoparticles, in that order.

The present study reveals and exposes the predominant factors as they affect the boundary layer of free convection flow and heat transfer of nanofluids. Moreover, the high level of accuracy and versatility of differential transformation method-Padé approximate technique has been demonstrated. It is hoped that the present study will enhance the understanding as it provides physical insights into the free convection boundary-layer problems.

## References

- [1] Schmidt, E., and Beckmann, W., "Das Temperatur-und Geschwindigkeitsfeld vor Einer Wärme Abgebenden Senkrechten Platte bei Natürlicher Convection", *Tech. Mech. U. Thermodynamik*, Bd. 1, Vol. (10) (1930), 341-349, cont. Bd. Vol. 1, No. 11, pp. 391- 406, (1930),
- [2] Ostrach, S., "An Analysis of Laminar Free-convection Flow and Heat Transfer about a Flat Plate Parallel to the Direction of the Generating Body Force", *NACA Report*, 1111, (1953).
- [3] Sparrow, E.M., and Gregg, J.L., "Laminar Free Convection from a Vertical Plate with Uniform Surface Heat Flux", *Trans. ASME*. Vol. 78, pp. 435-440, (1956).
- [4] Lefevre, E.J., "Laminar Free Convection from a Vertical Plane Surface", 9th Intern. Congress on Applied Mechanics, Brussels, Paper I, 168 (1956).
- [5] Sparrow, E.M., and Gregg, J.L., "Similar Solutions for Free Convection from a Nonisothermal Vertical Plate, *Trans. ASME*. Vol. 80, pp. 379-386, (1958).
- [6] Stewartson, K., and Jones, L.T., "The Heated Vertical Plate at High Prandtl Number, *J. Aeronautical Sciences* 24, pp. 379-380, (1957).

- [7] Kuiken, H.K., "An Asymptotic Solution for Large Prandtl Number Free Convection", J. Engng. Math. Vol. 2, pp. 355-371, (1968).
- [8] Kuiken, H.K., "Free Convection at Low Prandtl Numbers", J. Fluid Mech. Vol. 37, pp. 785-798, (1969).
- [9] Eshghy, S., "Free-convection Layers at Large Prandtl Number", J. Applied Math. and Physics (ZAMP), Vol. 22, pp. 275 -292, (1971).
- [10] Roy, S., "High Prandtl Number Free Convection for Uniform Surface Heat Flux", Trans ASME. J. Heat Transfer, Vol. 95, pp. 124-126, (1973).
- [11] Kuiken, H.K., and Rotem, Z., "Asymptotic Solution for the Plume at very Large and Small Prandtl Numbers, J. Fluid Mech. Vol. 45, pp. 585-600, (1971).
- [12] Na, T.Y., and Habib, I.S., "Solution of the Natural Convection Problem by Parameter Differentiation, Int. J. Heat Mass Transfer, Vol. 17, pp. 457–459, (1974).
- [13] Merkin, J.H., "A Note on the Similarity Solutions for Free Convection on a Vertical Plate", J. Engng. Math. Vol. 19, pp. 189-201, (1985).
- [14] Merkin, J.H., and Pop, I., "Conjugate Free Convection on a Vertical Surface", Int. J. Heat Mass Transfer, Vol. 39, pp. 1527–1534, (1996).
- [15] Ali, F. M., Nazar, R., and Arifin, N. M., "Numerical Investigation of Free Convective Boundary Layer in a Viscous Fluid", the American Journal of Scientific Research, No. 5, pp. 13–19, (2009).
- [16] Motsa, S. S., Shateyi, S., and Makukula, Z., "Homotopy Analysis of Free Convection Boundary Layer Flow with Heat and Mass Transfer", Chemical Engineering Communications, Vol. 198, No. 6, pp. 783–795, (2011).
- [17] Motsa, S. S., Makukula, Z. G., and Shateyi, S., "Spectral Local Linearization Approach for Natural Convection Boundary Layer Flow", Hindawi Publishing Corporation Mathematical Problems in Engineering, Vol. 2013, Article ID 765013, 7 pages, (2013),
- [18] Ghotbi, A.R., Bararnia, H., Domairry, G., and Barari, A., "Investigation of a Powerful Analytical Method into Natural Convection Boundary Layer Flow", Communications in Nonlinear Science and Numerical Simulation, Vol. 14, No. 5, pp. 2222–2228, (2009).
- [19] Zhou, J.K., "Differential Transformation and its Applications for Electrical Circuits", Huazhong University Press, Wuhan, China, (1986) (in Chinese).
- [20] Yu, L.T., and Chen, C.K., "The Solution of the Blasius Equation by the Differential Transformation Method", Math. Comput. Modell, Vol. 28, pp. 101–111, (1998).
- [21] Kuo, B.L., "Thermal Boundary-layer Problems in a Semi-infinite Flat Plate by the Differential Transformation Method", Appl. Math. Comput. Vol. 153, pp. 143–160, (2004).

- [22] Kuo, B. L., "Application of the Differential Transformation Method to the Solutions of the Free Convection Problem", *Applied Mathematics and Computation*, Vol. 165, pp. 63–79, (2005).
- [23] Rashidi, M. M., Laraqi, N., and Sadri, S. M., "A Novel Analytical Solution of Mixed Convection about an Inclined Flat Plate Embedded in a Porous Medium using the DTM-Pade, *International Journal of Thermal Sciences*, Vol. 49, No. 12, pp. 2405-2412, (2010).
- [24] El-Zahar, E. R., "Applications of Adaptive Multi-step Differential Transform Method to Singular Perturbation Problems Arising in Science and Engineering", *Applied Math. Inf. Sci.*, Vol. 9, pp. 223-232, (2015).
- [25] Erturk, V. S., Odibat, Z.M., and Momani, S., "The Multi-step Differential Transform Method and its Application to Determine the Solutions of Nonlinear Oscillators", *Adv. Applied Math. Mechan.* Vol. 4, pp. 422-438, (2012).
- [26] Gokdogan, A., Merdan, M., and Yildirim, A., "Adaptive Multi-step Differential Transformation Method to Solving Nonlinear Differential Equations", *Math. Comput. Modell.* Vol. 55, pp. 761-769, (2012a).
- [27] Gokdogan, A., Merdan, M., and Yildirim, A., "A Multistage Differential Transformation Method for Approximate Solution of Hantavirus Infection Model", *Commun. Nonlinear Sci. Numerical Simulat.* Vol. 17, pp. 1-8, (2012b).
- [28] Akbar, N. S., and Butt, A. W., "Ferro-magnetic Effects for Peristaltic Flow of Cu-water Nanofluid for Different Shapes of Nano-size Particles. *Appl. Nanosci.* Vol. 6, pp. 379-385, (2016),
- [29] Sheikholeslami, M., and Bhatti, M. M., "Free Convection of Nanofluid in the Presence of Constant Magnetic Field Considering Shape Effects of Nanoparticles", *International Journal of Heat and Mass Transfer*, Vol. 111, pp. 1039-1049, (2017).
- [30] Ul Haq, R., Nadeem, S., Khan, Z.H., and Noor, N.F.M., "Convective Heat Transfer in MHD Slip Flow Over a Stretching Surface in the Presence of Carbon Nanotubes", *Physica B*, Vol. 457, pp. 40-47, (2015).
- [31] Talley, L. D., Pickard, G. L., Emery, W. J., and Swift, J. H., "Descriptive Physical Oceanography", *Physical Properties of Sea Water*, Sixth Ed., Elsevier Ltd, pp. 29–65, (2011).
- [32] Pastoriza-Gallego, M., Lugo, L., Legido, J., and Piñeiro, M., "Thermal Conductivity and Viscosity Measurements of Ethylene Glycol-based Al<sub>2</sub>O<sub>3</sub> Nanofluids", *Nanoscale Res Lett.*, Vol. 6, pp. 1-11, (2011).
- [33] Aberoumand, S., and Jafarimoghaddam, A., "Experimental Study on Synthesis, Stability, Thermal Conductivity and Viscosity of Cu–engine Oil Nanofluid", *Journal of the Taiwan Institute of Chemical Engineers*, Vol. 71, pp. 315–322, (2017).
- [34] Kuiken, H. K., "On Boundary Layers in Fluid Mechanics that Decay Algebraically along Stretches of Wall that are not Vanishingly Small", *IMA Journal of Applied Mathematics*, Vol. 27, No. 4, pp. 387–405, (1981).



- [35] Ghadikolaei, S.S., Hosseinzadeh, Kh., Ganji, D.D., and Jafari, B., "Nonlinear Thermal Radiation Effect on Magneto Casson Nanofluid Flow with Joule Heating Effect Over an Inclined Porous Stretching Sheet", *Case Studies in Thermal Engineering*, Vol. 12, pp. 176–187, (2018).
- [36] Hosseinzadeh, Kh., Afsharpanah, F., Zamani, S., Gholinia, M., and Ganji, D.D., "A Numerical Investigation on Ethylene Glycol-titanium Dioxide Nanofluid Convective Flow Over a Stretching Sheet in Presence of Heat Generation/absorption", *Case Studies in Thermal Engineering*, Vol. 12, pp. 228–236, (2018).
- [37] Sheikholeslami, M., Nimafar, M., and Ganji, D.D., "Nanofluid Heat Transfer between Two Pipes Considering Brownian Motion using AGM", *Case Studies in Thermal Engineering*, Vol. 56, Issue. 2, pp. 277-283, (2017).
- [38] Ghadikolaei, S.S., Hosseinzadeh, Kh., and Ganji, D.D., "Analysis of Unsteady MHD Eyring-Powell Squeezing Flow in Stretching Channel with Considering Thermal Radiation and Joule Heating Effect using AGM", *Case Studies in Thermal Engineering*, Vol. 10, pp. 579-594, September (2017).
- [39] Rahimi, J., Ganji, D.D., Khaki, M., and Hosseinzadeh, Kh., "Solution of the Boundary Layer Flow of an Eyring-Powell Non-Newtonian Fluid Over a Linear Stretching Sheet by Collocation Method", *Alexandria Engineering Journal*, Vol. 56, Issue. 4, pp. 621-627, December (2017).

## Nomenclature

$c_p$	specific heat capacity
$k$	thermal conductivity
$m$	shape factor
$Pr$	Prandtl number
$u$	velocity component in x-direction
$v$	velocity component in z-direction
$y$	axis perpendicular to plates
$x$	axis along the horizontal direction
$y$	axis along the vertical direction

## Symbols

$\beta$	volumetric extension coefficients
$\rho$	density of the fluid
$\mu$	dynamic viscosity
$\eta$	similarity variable
$\lambda$	sphericity
$\phi$	volume fraction or concentration of the nanofluid
$\theta$	Dimensionless temperature

## Subscript

f	fluid
s	solid
nf	nanofluid